HHS Public Access

Author manuscript

Cell Metab. Author manuscript; available in PMC 2018 August 01.

Published in final edited form as:

Cell Metab. 2017 August 01; 26(2): 394–406.e6. doi:10.1016/j.cmet.2017.07.009.

Acetyl CoA Carboxylase Inhibition Reduces Hepatic Steatosis But Elevates Plasma Triglycerides in Mice and Humans: A Bedside to Bench Investigation

Chai-Wan Kim[1], **Carol Addy**[3], **Jun Kusunoki**[3], **Norma N. Anderson**[1], **Stanislaw Deja**[2], **Xiaorong Fu**[2], **Shawn C. Burgess**[2], **Cai Li**[3], **Manu Chakravarthy**[3], **Steve Previs**[3], **Stuart Milstein**[4], **Kevin Fitzgerald**[4], **David E. Kelley**[3], and **Jay D. Horton**[1,5,*]

[1]Department of Internal Medicine and Molecular Genetics, University of Texas Southwestern Medical Center, Dallas, TX 75390-9046

[2]Advanced Imaging Research Center and Department of Pharmacology, University of Texas Southwestern Medical Center, Dallas, TX 75390, USA

[3]MRL, 2000 Galloping Hill Road, Kenilworth, NJ 07033

[4]Alnylam Pharmaceuticals, 300 Third Street, Cambridge, MA 02142

SUMMARY

Inhibiting lipogenesis prevents hepatic steatosis in rodents with insulin resistance. To determine if reducing lipogenesis functions similarly in humans, we developed MK-4074, a liver-specific inhibitor of acetyl-CoA carboxylase (ACC1) and (ACC2); enzymes that produce malonyl-CoA for fatty acid synthesis. MK-4074 administered to subjects with hepatic steatosis for 1 month lowered lipogenesis, increased ketones, and reduced liver triglycerides by 36%. Unexpectedly, MK-4074 increased plasma triglycerides by 200%. To further investigate, mice that lack ACC1 and ACC2 in hepatocytes (ACC dLKO) were generated. Deletion of ACCs decreased polyunsaturated fatty acid (PUFA) concentrations in liver due to reduced malonyl-CoA, which is required for elongation of essential fatty acids. PUFA deficiency induced SREBP-1c, which increased GPAT1 expression and VLDL secretion. PUFA supplementation or siRNA-mediated knockdown of GPAT1 normalized plasma triglycerides. Thus, inhibiting lipogenesis in humans reduced hepatic steatosis, but inhibiting ACC resulted in hypertriglyceridemia due to activation of SREBP-1c and increased VLDL secretion.

[*]Correspondence: jay.horton@utsouthwestern.edu.
[5]Lead Contact

AUTHOR CONTRIBUTIONS

Study concept and design, C-W. K., C.L., D.K., and J.D.H.; Acquisition of data, C-W. K., C.A., J.K., N.N.A., X.R, S.D., S.M., M.C., C.L., S.P.; Analysis and interpretation of data, C-W. K., C.L., K.F., S.P., S.C.B, M.C., D.K., and J.D.H. Statistical analysis, C-W. K., and S.P., M.C.; Technical support, K.F.; Drafting of the manuscript, C-W. K., C.L., D.K., and J.D.H.

SUPPLEMENTAL INFORMATION

Supplemental Information includes 3 tables and 4 figures.

Graphical Abstract

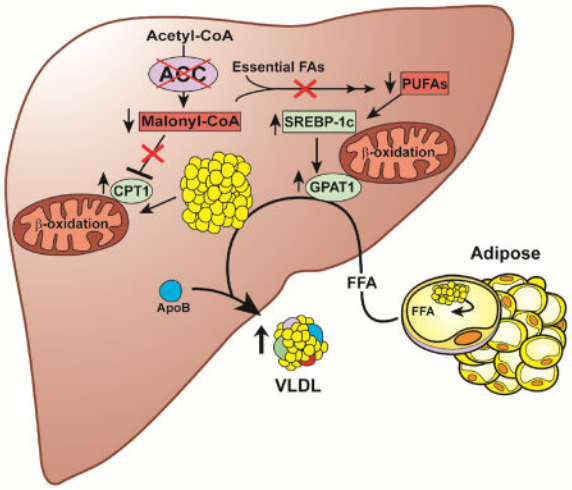

Kim et al. describe an inhibitor of acetyl-CoA carboxylase (ACC) 1 and 2 that reduces liver triglycerides in individuals with fatty livers, but increases plasma triglycerides. In mice lacking ACCs, reduced malonyl-CoA levels suppress polyunsaturated fatty acid synthesis leading to increased SREBP-1c and GPAT1 expression, increased VLDL secretion, and hypertriglyceridemia.

Keywords

Hepatic steatosis; acetyl-CoA carboxylase; inhibitors; lipogenesis; hypertriglyceridemia; SREBPs; malonyl-CoA

INTRODUCTION

Nonalcoholic fatty liver disease (NAFLD) encompasses a continuum of liver abnormalities that includes excess triglyceride (TG) accumulation (hepatic steatosis), ballooning degeneration, inflammation, fibrosis, and cirrhosis (Browning and Horton, 2004). Hepatic steatosis affects ~33% of adults in the U.S. and is strongly associated with obesity, insulin resistance, and type 2 diabetes mellitus (Browning et al., 2004). Of those individuals with hepatic steatosis, it is estimated that ~15–20% will progress to nonalcoholic steatohepatitis, and ~10–15% of these individuals will progress to cirrhosis (Cohen et al., 2011). Despite the large disease burden, the only available therapy for NAFLD is weight loss and possibly vitamin E supplementation in select individuals (Chalasani et al., 2012). Pioglitazone has also shown promising results and reduces liver TGs and fibrosis but is not currently approved for the treatment of NAFLD (Bajaj et al., 2003; Belfort et al., 2006; Cusi et al., 2016; Musso et al., 2017; Promrat et al., 2004; Sanyal et al., 2010).

The underlying pathogenesis of NAFLD is incompletely understood, but the elucidation of the underlying metabolic alterations that lead to excess TGs in liver may result in therapeutic opportunities for treatment. Studies in animal models and humans with NAFLD have consistently demonstrated the presence of underlying insulin resistance (Browning et al.,

2004). Therapies that improve insulin resistance also reduce liver TGs (Bajaj et al., 2003; Belfort et al., 2006; Khan et al., 2002; Musso et al., 2010; Promrat et al., 2004; Sanyal et al., 2010). The molecular consequences of hepatic insulin resistance have been only partially defined, but one key abnormality is the paradoxical stimulation of hepatic *de novo* lipogenesis (DNL) in rodent models of NAFLD (Moon et al., 2012; Shimomura et al., 1999a). In mouse models of hepatic steatosis, hyperinsulinemia increases the expression of SREBP-1c, a transcription factor that activates all genes encoding enzymes required for the synthesis of fatty acids and the first enzyme in TG synthesis (Horton et al., 2002; Shimomura et al., 1999b). The genetic ablation of *Scap*, a protein required for SREBP activation, ameliorated hepatic steatosis and reduced plasma TGs in rodent models of insulin resistance and hepatic steatosis (Moon et al., 2012). These studies demonstrated that activation of the lipogenic pathway in liver is a key metabolic alteration required for the development of hepatic steatosis in insulin resistant states and may contribute to the associated hypertriglyceridemia frequently associated with NAFLD.

The relative importance of activation of DNL in humans with NAFLD has been debated inasmuch as rodents have higher absolute rates of hepatic DNL compared to humans (Aarsland et al., 1997; Shimomura et al., 1999a; Wolfe, 1998). In addition, Parks and colleagues (Donnelly et al., 2005) have shown that ~60% of the TG that accumulated in liver in humans with NAFLD is derived from adipose tissue, while only ~25% is derived from DNL. Nevertheless, it has been established that humans with NAFLD have significantly higher rates of hepatic DNL compared to lean individuals (Donnelly et al., 2005; Fabbrini et al., 2008; Lambert et al., 2014), thus it is possible that inhibiting DNL might reduce hepatic steatosis in humans as it did in rodents.

DNL is carried out in the cytosol by three enzymes, ATP citrate lyase, acetyl-CoA carboxylase (ACC), and fatty acid synthase (FASN). ATP citrate lyase produces acetyl-CoA, the substrate for acetyl-CoA carboxylase (ACC), which produces malonyl-CoA. Fatty acid synthase, a multifunctional enzyme, utilizes acetyl-CoA and malonyl-CoA to ultimately generate palmitate (C16:0). ACC is the first committed enzyme in the DNL pathway and two isozymes, ACC1 and ACC2, exist in mammals (Thampy and Wakil, 1988a, b). The two ACC isoforms have generally been regarded as having distinct physiological roles: ACC1, a cytosolic enzyme is committed to the rate-limiting step in DNL; and ACC2, a mitochondrial membrane associated enzyme that generates malonyl-CoA primarily to allosterically inhibit of carnitine palmitolytransferase (CPT-1), which is responsible for long chain fatty acid transport into mitochondria (Abu-Elheiga et al., 2000). Based on this biochemistry, it was expected that combined ACC1 and ACC2 inhibition would result in reduction of DNL and enhanced fatty acid oxidation (FAO), leading to decreased TGs in liver.

Studies in mice support the proposed benefit of ACC inhibition if confined to liver inasmuch as germline deletion of ACC1 resulted in embryonic lethality (Abu-Elheiga et al., 2005). ACC1 liver-specific knockout mice were generated independently by Harada et al. (Harada et al., 2007) and Mao *et al.* (Mao et al., 2006). Both groups showed that the ACC1 knockout mice fed a high sucrose diet had reduced hepatic DNL compared to controls. ACC2 knockout mice have been produced by two independent groups but with conflicting results. Mice with the germline deletion of ACC2 generated by Abu-Elheiga *et al.* (Abu-Elheiga et

al., 2003) had higher rates of FAO in muscle and heart resulting in lower body fat (Abu-Elheiga et al., 2003; Choi et al., 2007). In contrast, ACC2 knockout mice generated by Olson *et al.* (Olson et al., 2010) had virtually no alteration in fat metabolism (Olson et al., 2010). Nevertheless, the combined data from the ACC knockout mouse studies suggested that a duel inhibitor of hepatic ACCs may lower liver TGs.

In the current studies, we present findings from pharmacological inhibition of ACCs obtained by administration of MK-4074, a potent liver-targeted inhibitor of ACC1 and ACC2. In cellular assays of cultured hepatocytes, preclinical animal models, and clinical studies, the administration of MK-4074 inhibited DNL and enhanced hepatic FAO. Importantly, MK-4074 significantly reduced hepatic TG content in preclinical studies. The goal of the current investigations was to determine whether MK-4074 reduced hepatic fat content in humans with hepatic steatosis. The data presented confirm that inhibition of ACC does substantially improve hepatic steatosis, even after only one month of administration. However, an unexpected finding within this exploratory study was that liver-targeted ACC inhibition by MK-4074 was also associated with an unexpected rise in plasma TGs.

Hepatic steatosis is commonly associated the metabolic syndrome and elevated plasma TGs (Chalasani et al., 2012; Grundy et al., 2004). Reductions in hepatic steatosis achieved by dietary restriction and weight loss have been associated with corresponding reductions in plasma TGs (Cohen et al., 2011). Based on previous rodent studies in which Scap was inhibited, the a priori expectation was that if the pharmacological inhibition of ACC reduced hepatic TGs, it would also lead to a lowering or at least neutral effect on plasma TGs. The unexpected finding that the reduction of hepatic steatosis by ACC inhibition was associated with a clinically as well as statistically significant rise in plasma TGs, led to the undertaking of a “bedside to bench” investigation to determine the underlying mechanism responsible for this seemingly paradoxical effect.

RESULTS

Identification and Characterization of MK-4074, a Liver-targeted Small Molecule Inhibitor of ACC1 and ACC2

High throughput screening for drug candidates and then subsequent medicinal chemistry efforts on initial leads yielded MK-4074, which is a potent and specific human ACC1/2 dual inhibitor (Figure 1A). MK-4074 strongly inhibited both ACC1 and 2 with IC50 values of approximately 3 nM. MK-4074 is highly liver-specific because it is a substrate of organic anion transport proteins (OATP) transporters that are present only in hepatocytes and excretion of MK-4074 from hepatocytes into bile is dependent on the MRP2 efflux transporter. These factors, together with low cell penetrance, imbued MK-4074 with liver targeting. Tissue distribution studies of [^{14}C] MK-4074 in mice indicated that MK-4074-related radioactivity was highly localized to liver after oral administration with an estimated liver/plasma ratio of ~33–37 at 1 and 4 hours following dosing (Figure S1).

In male KKAy mice, a mouse model of obesity, type II diabetes and fatty liver, a single oral dose of MK-4074 (0.3 to 3 mg/kg) significantly decreased DNL in a dose-dependent manner with an ID_{50} value of 0.9 mg/kg 1 hour post administration (Figure 1B). In a time-course

study, MK-4074 at 30 mg/kg P.O. reduced hepatic DNL by 83%, 70%, and 51% at 4, 8, and 12 hours post dose, respectively (Figure 1C). Single oral doses of MK-4074 at 30 and 100 mg/kg significantly increased plasma total ketones, a surrogate biomarker for hepatic FAO, by 1.5~3-fold for up to 8 hours (Figure 1D).

In an independent diet-induced model of hepatic steatosis, male C57BL/6J mice were fed a high fat/high sucrose (HF/HS) diet for 7 weeks and administered MK-4074 or vehicle orally at 10 and 30 mg/kg/day for 4 weeks prior to study. Mice fed chow and given the dosing vehicle during the same period were compared to these groups as controls. The hepatic TG content in vehicle-treated mice on the HF/HS diet increased 11-fold compared to mice on chow. The HF/HS diet-induced increase in TG content was significantly reduced by 46% and 36% in mice given MK-4074 at 10 and 30 mg/kg/day Q.D., respectively (Figure 1E and 1F).

Phase 1 Studies with MK-4074 in Healthy Subjects

Based on the success of the initial animal studies, Phase 1 studies in humans were conducted in healthy individuals. As detailed in Experimental Procedures, research subjects had DNL induced by oral administration of fructose loading and the rate of DNL was estimated using a stable isotope labeling method, as described (Hudgins et al., 2000). MK-4074 administered as a single dose of 140 mg, or as a divided dose (70 mg b.i.d.) to healthy young male subjects resulted in inhibition of fractional DNL by approximately 96% and 91%, respectively, relative to placebo (Figure 2A). Multiple-dose administration of MK-4074, 140 mg for 7 days resulted in maximal DNL inhibition, suggesting that maximal or near maximal inhibition of ACC1 resulted at the evaluated doses. Fructose loading stimulates DNL, which leads to suppressed levels of plasma ketones. To examine the potential effect of MK-4074 on hepatic FAO, separate studies were carried out in the fasted and fed state. Single-dose administration of MK-4074 (200 mg) to healthy subjects resulted in ~2.5-fold increase in acetoacetate and β-hydroxybutyrate relative to placebo in the fasted state and smaller but significant increases were measured in the fed state (Figure 2B).

Administration of MK-4074 to Subjects with Hepatic Steatosis

The Phase 1 data confirmed that MK-4074 inhibited ACC1 and ACC2 in humans, and prompted a small study to assess the effect of 4 weeks treatment with MK-4074 on hepatic steatosis. Thirty male or female patients between the ages of 18 and 60 (Table S1 and S2) were randomized to: 1) twice daily 200 mg dose of MK-4074; 2) once daily 30 mg doses of pioglitazone; or 3) placebo for 4 weeks. A pioglitazone arm was included as a comparator since it has previously been shown to reduce liver TGs and fibrosis (Bajaj et al., 2003; Belfort et al., 2006; Cusi et al., 2016; Musso et al., 2017; Promrat et al., 2004; Sanyal et al., 2010). Hepatic fat content was assessed using magnetic resonance imaging (MRI) prior to first administration and following 4 weeks of treatment. Compared with baseline measurements, MK-4074 decreased hepatic fat by 36%, pioglitazone decreased hepatic fat by 18% and subjects on placebo had an 8.6% increase in hepatic fat (Figure 3A, Table S3). The difference in hepatic fat reduction between MK-4074 and pioglitazone was statistically significant, as was the difference between MK-4074 and placebo.

Unexpectedly, plasma TGs were significantly increased in those administered MK-4704 relative to pre-dose baseline, an effect not observed in either the placebo or pioglitazone arms (Figure 3B). Four weeks of treatment with MK-4074 increased the mean plasma TGs concentrations by approximately 2-fold (average baseline 170 mg/dL and at the end of 4 weeks treatment 325 mg/dl). Additional analyses of lipoproteins carried out in the MK-4074 treated subjects revealed significant increases in TGs in VLDL, LDL, and HDL, whereas no changes were detected in the lipoproteins from pioglitazone or placebo treated subjects (Figure 3C).

Generation of ACC1 and ACC2 Liver-specific Knockout Mice to Investigate the Mechanism of Hypertriglyceridemia Induced by ACC Inhibition

A mouse line with floxed ACC1 allele was generated by inserting the bacterial neomycin resistance gene (neo) flanked by loxP sites between exon 26 and 27 of the mouse *Acc1*, and an additional loxP site was inserted between exon 21 and 22. The construct was designed to generate successive stop codons following deletion. The floxed ACC2 mouse line was obtained from Jackson labs (01342, B6N;129S-*Acacb*$^{tm1.1Lowl}$/J). ACC1 and ACC2 hepatocyte-specific double knockout mice (ACC dLKO) were generated by breeding lines of floxed ACC1 allele and ACC2 allele mice with albumin-CRE transgenic mice (Moon et al., 2012).

To confirm ACCs were deleted, liver tissue lysates were prepared from wild type, hepatocyte-specific ACC1 knockout (ACC1 LKO), hepatocyte-specific ACC2 knockout (ACC2 LKO), and ACC dLKO mice. Immunoblots were performed using anti-mouse ACC1 and anti-mouse ACC2 rabbit polyclonal antibodies that were generated using N-terminal polypeptides of ACC1 and ACC2. As shown in Figure S2A, no ACC1 or ACC2 protein was detected in livers of ACC1 LKO and ACC2 LKO, respectively. Similarly, neither ACC protein was detected in livers of ACC dLKO mice.

We next confirmed that deletion of ACCs in hepatocytes reduced overall rates of fatty acid synthesis in liver. First, *in vivo* rates of hepatic fatty acid synthesis were measured after injecting mice with $^{3}H_2O$. Using this technique, rates of fatty acid synthesis were reduced by 80% (Figure S2B). The absolute rate of fatty acid synthesis in these studies was not zero because the study includes whole liver, which includes cells other than hepatocytes and tritium will label elongated fatty acids derived from the diet or made in the peripheral tissues. Similarly, the deletion of ACC1 and ACC2 reduced malonyl-CoA levels by ~80% in liver (Figure S2C). The residual malonyl-CoA measured was likely from non-hepatocytes present in the whole liver homogenates. To confirm that the deletion of ACCs resulted in no fatty acid synthesis in hepatocytes, we measured fatty acid synthesis using [^{3}H]acetate as the tracer in primary hepatocytes derived from ACC1 LKO, ACC2 LKO, and ACC dLKO mice. Synthesis rates were then calculated by measuring the amount of fatty acids with ^{3}H incorporation at 3 hours. The deletion of both ACCs resulted in rates of newly synthesized fatty acids incorporated into TGs and phospholipids that were below the limits of detection in the primary hepatocytes (Figure S2D). Ketone bodies (total ketones and 3-hydroxybutyrate) were measured in plasma as a surrogate of FAO. Total ketones and 3-

hydroxybutyrate concentrations were 2.5-fold higher in plasma from ACC dLKO mice compared to that from wild type mice (Figure S2E).

Consistent with previous reports, liver TG concentrations were reduced by 40% in ACC dLKO mice fed chow (Figure 4A) (Harada et al., 2007; Mao et al., 2006). We also fed mice a western diet for one month or a high fat diet for four months to determine if ACC inhibition was sufficient to ameliorate the hepatic steatosis that results from these dietary manipulations. Feeding wild type mice the western diet increased their liver TGs to ~95 mg/g and feeding the high fat diet increased liver TGs to ~80 mg/g. However, liver TGs in ACC dLKO mice fed either diet remained less than 10 mg/g, the amount present in livers of wild type mice fed chow (Figure 4B, 4C).

We also tested whether the deletion of ACCs was sufficient to prevent the development of hepatic steatosis in *ob/ob* mice, an extreme mouse model of obesity, insulin resistance, and fatty liver. Deletion of ACCs from *ob/ob* mice did not result in a change in body weight. However, as shown in Figure 4D, deletion of ACCs from *ob/ob* mice completely prevented the development of hepatic steatosis and liver TGs remained at ~10 mg/g. Loss of lipids and smaller lipid droplets in hepatocytes as a result of deleting ACCs was also confirmed by histological examination (Figure S3).

As was found in the human studies with MK-4074 and despite the normalization of liver TGs in ACC dLKO mice under multiple conditions that induce hepatic steatosis, plasma TGs levels were paradoxically increased under all conditions studied. Plasma TG levels were markedly elevated in ACC dLKO mice fed chow, western, or high fat diets (Figure 4E–4G). Similarly, plasma TGs from *ob/ob* mice that lack ACCs were 3-fold higher than *ob/ob* controls (Figure 4H). Plasma lipoproteins from wild type and ACC dLKO mice fed chow were separated by FPLC and TG concentrations were measured. As shown in Figure 4I, the TG measured in plasma was carried in VLDL-sized particles.

To define the molecular mechanism responsible for the development of hypertriglyceridemia, we used microarrays to identified genes with altered expression in livers ACC dLKO mice. These studies revealed that the mRNA levels of genes regulated by SREBP-1c were all significantly increased in ACC dLKO livers (data not shown); therefore, SREBP-1 protein levels were measured in livers from wild type and ACC dLKO mice. As shown in Figure 5A, the amount of transcriptionally active nuclear form and membrane bound precursor SREBP-1 protein levels were significantly increased in livers of ACC dLKO mice. SREBP-1c activation was also found in ACC dLKO mice fed a high fat diet (Figure S3C), a diet that more closely recapitulates steatosis in humans. We then confirmed the results from the microarray by measuring the mRNA levels of known SREBP-1c regulated genes by quantitative PCR in livers from wild type and ACC dLKO mice (Figure 5B). *Srebp-1c* is transcriptionally activated by itself through a feed-forward mechanism (Horton et al., 2002). Consistent with the increase in SREBP-1 protein, the mRNA levels encoding SREBP-1c was increased ~1.8-fold. Similarly, the mRNAs levels for all SREBP-1c-regulated genes in the DNL pathway were increased 5- to 35-fold. The mRNA levels of an additional SREBP-regulated gene, PNPLA3, were increased ~25-to 60-fold.

Polymorphisms in *PNPLA3* have been associated with hepatic steatosis, NASH, and cirrhosis in humans (Cohen et al., 2011).

We have shown previously that SREBP-1 is tonically suppressed by polyunsaturated fatty acids (PUFAs) endogenously synthesized from essential fatty acids in liver (Moon et al., 2009). One possibility for the aberrant activation of SREBP-1 was a relative reduction in PUFAs that could result from a deficiency of malonyl-CoA in the ACC dLKO mouse livers. Carbons derived from malonyl-CoA are required for the elongation of essential fatty acids linoleic (C18:2, n-6) and linolenic (C18;3, n-3) to form PUFAs (Moon and Horton, 2003). To test the possibility that ACC dLKO mice are deficient in PUFAs, we quantified the fatty acid composition in livers of wild type and ACC dLKO mice using gas chromatography. As shown in Figure 6A, the amount of palmitate (C16:0) and stearate (C18:0) were significantly lower in livers of ACC dLKO mice likely as a result of the lower rates of DNL. The major PUFAs present in wild type livers are arachidonic acid (ARA) (C20:4, n-6) and docosahexaenoic acid (DHA) (C22:6, n-3) and both potently suppress SREBP-1c (Moon et al., 2009). The concentrations of ARA and DHA were reduced by 30% and 73%, respectively in livers from by ACC dLKO mice.

To determine whether the relative deficiency in PUFAs was responsible for the enhanced activation of SREBP-1, we fed ACC dLKO mice a diet supplemented with ARA and DHA to restore these PUFAs to levels measured in wild type mouse liver. This was accomplished by supplementing chow with 1% ARA and 0.4% DHA for 10 days. As shown in Figure 6A, supplementation of ARA and DHA restored the levels of these PUFAs to levels that were not significantly different than those measured in livers from wild type mice fed chow. ARA and DHA restoration was sufficient to reduce nuclear SREBP-1 protein to levels that were only slightly higher than that measured in wild type mice fed chow (Figure 6B). Similarly, the mRNA levels of SREBP-1c and its regulated genes were reduced to levels only slightly higher than that measured in livers of wild type mice fed chow (Figure 6C). It is likely that complete normalization of SREBP-1 and target gene levels was not obtained because not all PUFAs that were lower in the ACC dLKO livers could be re-supplemented. We next determined whether the reduction in SREBP-1 and its regulated genes altered the hypertriglyceridemia found in the plasma of ACC dLKO mice. As shown in Figure 6D, plasma TG concentrations in ACC dLKO mice were normalized by PUFA supplementation with no resulting increase in liver TGs (Figure 6E).

The above results suggested that SREBP-1 activation was required for the hypertriglyceridemia found in ACC dLKO mice. To further explore the underlying mechanism responsible for the hypertriglyceridemia, we first measured rates of TG secretion in wild type and ACC dLKO mice after injection of Triton WR 1339. As shown in Figure 7A, rates of TG secretion from ACC dLKO mice were 30% higher than that measured in wild type mice.

The TG secretion studies suggested that increased VLDL production was likely responsible for the hypertriglyceridemia associated with ACC inhibition. This was an unexpected finding given the marked suppression of DNL. However, previous studies have shown that a large proportion of TGs present in VLDL are derived from fatty acids derived from the

periphery (Donnelly et al., 2005). GPAT1 catalyzes the first committed step in TG synthesis in liver (Gonzalez-Baro et al., 2007) and the expression of GPAT1 was significantly increased as a result of SREBP-1c activation in ACC dLKO mice. GPAT1 could use fatty acids derived from the periphery to form TGs for incorporation into VLDL. To determine whether activation of GPAT1 was required for the development of hypertriglyceridemia in ACC dLKO mice, we used siRNA to reduce the expression of GPAT1 to the level measured in wild type mouse livers. A dose-response study was first carried out to establish the amount of siRNA required to suppress GPAT1 mRNA levels to that present in wild type mouse livers (data not shown). As shown in Figure 7B, injection of 7.5 mg/kg of GPAT1 siRNA to ACC dLKO mice reduced hepatic GPAT1 mRNA levels to that measured in livers from wild type mice. Normalization of GPAT1 expression in liver was sufficient to completely ameliorate the hypertriglyceridemia found in ACC dLKO mice (Figure 7C). The lowering of plasma TGs in in ACC dLKO administered the GPAT1 siRNA was not associated with an increase in liver TGs (Figure 7D) but was associated with increased plasma ketones (data not shown), suggesting that the FAs that were no longer secreted were oxidized.

DISCUSSION

Using a high throughput screen for inhibitors of ACC, we identified MK-4074, a potent and liver-specific inhibitor of human ACC1 and ACC2. MK-4074 administered to mice and humans markedly reduced DNL and increased surrogate measures of FAO. The administration of MK-4074 to humans with hepatic steatosis reduced liver fat on average by 36%. The reduction in liver fat was greater than that achieved by the administration of pioglitazone and for the first time demonstrated that lowering DNL through the inhibition of ACC effectively reduces liver TGs in humans. Unfortunately, while there was a reduction in liver TG content, plasma TGs were significantly increased in those individuals who received MK-4074. Studies in ACC knockout mice demonstrated the increase in plasma TGs was secondary to a relative reduction in PUFAs, which resulted in increased SREBP-1c activation, elevated GPAT1 expression, and increased VLDL production from liver.

High rates of lipogenesis are associated with the development of hepatic steatosis in mice and humans (Cohen et al., 2011). Whether lowering DNL in humans could effectively reduce hepatic steatosis in humans had not been previously demonstrated. Here, reducing lipogenesis by inhibiting ACC led to a significant reduction in liver TGs. The positive impact on liver TGs is likely a combined effect of reducing malonyl-CoA production through inhibiting ACC, which not only reduces DNL but also leads to an increase in FAO by increasing CPT1 activity.

To date, the most promising drug to potentially treat NAFLD has been pioglitazone. Several studies have demonstrated a significant reduction in liver fat following the administration of pioglitazone (Bajaj et al., 2003; Belfort et al., 2006; Cusi et al., 2016; Musso et al., 2017; Promrat et al., 2004; Sanyal et al., 2010). Pioglitazone increases insulin sensitivity, which reduces activation of SREBP-1c and subsequently lowers rates of lipogenesis in liver (Araujo et al., 2016; Bell et al., 2012). Reduction in hepatic fat following pioglitazone therapy appears to be associated with histologic improvement in patients with NASH.

Whether the reduction in liver fat associated with ACC inhibition would similarly improve histologic evidence of NASH has not yet been investigated.

The unexpected observation from the human clinical trial associated with administration of MK-4074 was increased plasma TGs. One individual's plasma TGs rose to over 800 mg/dl (Figure 3B). We confirmed that the hypertriglyceridemia associated with MK-4074 was not an unexpected off-target effect of MK-4074 but that the hypertriglyceridemia was a direct consequence of the target engagement through studies in the ACC liver-specific knockout mice. The ACC knockout mice also developed marked hypertriglyceridemia when fed chow or challenged with a western or high fat diet. The underlying mechanism responsible for the hypertriglyceridemia in ACC dLKO mice was due to loss of malonyl-CoA, which is required to elongate essential fatty acids to form PUFAs (Figure 6A). We previously confirmed through the deletion of ELOVL5 that blocking endogenous synthesis of PUFAs from essential fatty acids leads to higher levels of SREBP-1c and fatty livers in mice (Moon et al., 2009). In ACC-deficient livers, activation of SREBP-1c induced the expression of GPAT1, which led to increased secretion of VLDL from liver. The increased SREBP-1c levels and hypertriglyceridemia were completely reversed in the ACC dLKO livers by restoring PUFAs levels by dietary supplementation (Figure 6). Similarly, plasma TGs were returned to normal levels in the ACC dLKO mice by lowering the expression of GPAT1 in liver to levels found in wild type mice (Figure 7).

The importance of GPAT1 activation and subsequent channeling of fatty acids into TGs for VLDL secretion is supported from previous studies in Scap deficient rodents. Inhibition of Scap, an escort protein required for the activation of SREBPs, completely prevented the development of hepatic steatosis in mice and hamsters but reduced VLDL secretion from liver resulting in lower plasma TGs (Moon et al., 2012). In contrast to inhibiting ACC, lowering lipogenesis through the inhibition of Scap lowered GPAT1 expression as a result of the loss of SREBP-1c. The mechanism by which GPAT1 activation in the absence of ACC activity channels fatty acids from the periphery into TGs destined for incorporation into VLDL for secretion from liver will require additional studies.

A second potentially significant consequence of ACC inhibition for the treatment of NAFLD is another consequence of SREBP-1c activation. SREBP-1c is the only known activator of PNPLA3 (Huang et al., 2010) and levels of PNPLA3 expression were increased ~20- to 60-fold in ACC dLKO livers. PNPLA3 belongs to a family of lipases and is located on lipid droplets in liver (He et al., 2010; Romeo et al., 2008). A polymorphism in *PNPLA3* is associated with the development of hepatic steatosis, NASH, cirrhosis, and hepatocellular carcinoma in humans (Cohen et al., 2011). This polymorphism is common and found in ~49% of Hispanics, ~23% of Caucasians, and ~18% of African Americans (Romeo et al., 2008). While the mechanism by which the *PNPLA3* polymorphism leads to NAFLD is not understood, studies by Hobbs and colleagues demonstrated that high levels of the mutant PNPLA3 protein are necessary for hepatic steatosis to develop in mice (Li et al., 2012; Smagris et al., 2015). If this finding translates to humans, the activation of *PNPLA3* that results from ACC inhibition could ultimately be detrimental even if DNL and liver TGs are lowered in those individuals who harbor the *PNPLA3* polymorphism.

Inhibition of DNL has also been accomplished through the inhibition or deletion of FASN. In contrast to both ACC and Scap inhibition, liver-specific inactivation of FASN in mice resulted in increased liver TGs (Chakravarthy et al., 2005). Semenkovich and colleagues subsequently showed that the deletion of FASN results in the loss of an endogenous PPARα ligand, which reduces PPARα activity and the expression of PPARα -regulated genes involved in FAO (Chakravarthy et al., 2009). A similar loss of a PPARα ligand might be expected in the ACC dLKO mice since flux through FASN was also inhibited. Indeed, we found the expression of PPARα-regulated genes, mitochondrial HMG-CoA synthase, ApoA5, ANGPL4, and CPT1a were also reduced in ACC dLKO livers as was CPT1a protein (Figure S4A, B, C). However, unlike what was reported in livers that lack FASN, ACC dLKO mice and humans administered MK-4074 had enhanced FAO. The principal difference in hepatic FAO between the FASN and ACC inhibition is that FASN knockout livers accumulate malonyl-CoA, which limits CPT1 activity; whereas ACC dLKO livers have low malonyl-CoA concentrations, which enhances CPT1 activity facilitating the entry of fatty acids into the mitochondria for oxidation. Administration of a synthetic PPARα ligand (WY14643) to mice increased plasma ketone bodies 2-fold in wild type mice, but they increased ~8-fold in ACC dLKO mice (Figure S4D). Administration of WY14643 also reduced plasma TGs in ACC dLKO mice to levels measured in wild type mice (Figure S4E). This suggests that the TGs normally destined for incorporation into VLDL for secretion were oxidized once PPARα activity was restored in ACC dLKO mice, even though GPAT1 mRNA levels in ACC dLKO mice remained elevated (data not shown). As described above, how the channeling of fatty acids between oxidation and secretion is regulated is not known but the localization of GPAT1 to the mitochondrial membrane opens the possibility that GPAT1 cooperates/interacts with CPT1 to regulate this channeling.

Previous reports suggested that plasma TG levels are increased following ACC inhibition. The germline deletion of ACC2 resulted in increased plasma TGs (Abu-Elheiga et al., 2001). It was suggested in this report that the increased serum TGs were due to the mobilization of TGs from peripheral organs due to the lack of malonyl-CoA, although no mechanistic studies were reported. However, a recent study by Harriman *et al.* (Harriman et al., 2016) reported the effects of ACC inhibition in rats using ND-630, an allosteric inhibitor of ACC dimerization. Consistent with the studies reported in this report, they found that ACC inhibition in DIO and Zucker diabetic rats significantly reduced liver TG content but also increased insulin sensitivity. In contrast to our studies in mice and humans, they found plasma TGs decreased after administration of the ACC inhibitor. The reason for the discrepancy is not clear at this time. It is possible the rat responds differently to ACC inhibition than mice and humans, that inhibition of ACC in peripheral tissues as well as liver results in changes that increase plasma VLDL clearance or catabolism, or that the ND-630 does not inhibit ACC activity to the same degree as MK-4074. Additional studies will be required to resolve this important issue.

The results reported here show for the first time that the inhibition of ACC in humans can significantly reduce liver TGs and that alternative strategies to reduce lipogenesis that also enhance FAO might be beneficial for the treatment of NAFLD. Unfortunately, we found liver inhibition of ACC resulted in a relative deficiency of PUFAs, which led to the activation of SREBP-1c, elevated GPAT1 expression, and hypertriglyceridemia. It may be

that not all individuals with NAFLD who are administered an ACC inhibitor will manifest significant hypertriglyceridemia and the degree of hypertriglyceridemia may be modulated by the amount of PUFAs ingested or the individuals propensity to develop hypertriglyceridemia; however, the resulting activation of SREBP-1c, which also induced PNPLA3 expression could also be detrimental to those who carry the *PNPLA3* polymorphism associated with NAFLD and cirrhosis. Combined, the findings of elevated plasma TGs and elevated PNPLA3 expression likely precludes the use of a liver-specific ACC inhibitors for the treatment of NAFLD. Although, the demonstration that inhibiting DNL lowers hepatic fat in humans does support continued efforts to develop alternative strategies to lower DNL for the treatment of NAFLD. One such approach could be through the inhibition of Scap in liver, which reduces DNL but also reduces the expression of GPAT1 and PNPLA3.

STAR METHOD

Contact for Reagent and Resource Sharing

Further information and requests for resources and reagents should be directed to and will be fulfilled by the Lead Contact, Jay Horton (jay.horton@utsouthwestern.edu).

EXPERIMENTAL MODEL AND SUBJECT DETAILS

Mice—All experiments performed at Tsukuba Research Institute involving animals were carried out in strict accordance with institutional guidelines governing the use of laboratory animals in research and were reviewed and approved by Institutional Animal Care and Use Committee (APS numbers 07J0040, 06J0048, 06J0091, and 07J0060) at Banyu Pharmaceutical Co., Ltd (Tsukuba, Japan). Mice were housed at 23 °C and under a 12-hour light cycle (7AM on, 7PM off). All animal experiments in UT Southwestern were performed with approval of the Institutional Animal Care and Research Advisory Committee (#2015-101135). Mice were housed at 72°F and under a 12-hour light cycle light cycle (6AM on, 6PM off).

Mouse Studies with MK-4074—Studies were performed in male KKAy mice or C57BL/6J mice (from CLEA Japan, Inc.). KKAy mice were fed a chow diet (CE-2, CLEA Japan Inc.) while C57BL/6J mice were fed a high fat diet (45% fat, Research Diets D12451) for 3 weeks prior to study. Mice were treated for 7 days with vehicle (distilled water, 0.2 mL/mouse) before MK-4074 administration to acclimate mice to oral dosing. Animals were drug naive at the time of study. Mice were housed individually. Male KKAy mice (n=10–11/group) were administered a single oral dose of MK-4074 (0.3 to 3 mg/kg) prior to liver slice studies. Male KKAy mice (n=5/group) were administered a single oral dose of MK-4074 (3 to 30 mg/kg) prior to measurement of liver DNL rates. Male KKAy mice (n=8/group) were administered a single oral dose of MK-4074 (10 to 100 mg/kg) and plasma ketone bodies were measured at the indicated times. Male C57BL/6J mice (n=5, veh; n=10, MK-4074) were fed chow or a high fat/high sucrose (HF/HS) diet for 7 weeks and vehicle or MK-4074 was administered orally (10 or 30 mg/kg/day) for 4 weeks prior to study.

***Ex Vivo* Determinations of DNL in Mice—**Male KKAy mice described above were used to evaluate PD effects of MK-4074. To measure *ex vivo* hepatic DNL, MK-4074 was orally administered to KKAy mice, and liver slices prepared immediately after dissection at indicated time points and incubated in DMEM with 0.5 mM ^{14}C-acetate for 60 min at 37°C. The lipid fraction was extracted from the liver slices with $CHCl_3$-methanol mixture (2:1) and saponified. The radioactivity in the saponified lipid fraction was measured using a scintillation counter.

ACC1 and ACC2 Liver-specific Knockout Mice—ACC1 floxed alleles were generated by inserting the bacterial neomycin resistance gene (neo) flanked by loxP sites between exons 26 and 27 of the mouse *Acc1* gene, and an additional loxP site was inserted between exon 21 and 22 (Figure S2). *Acc2*$^{f/f}$ mice were purchased from Jackson labs. ACC1 and ACC2 liver-specific double knockout mice was generated by crossing *Acc1*$^{f/f}$and *Acc2*$^{f/f}$ mice with albumin-CRE transgenic mice (ACC dLKO). To obtain ACC dLKO mice in *ob/ob* background, ACC dLKO mice were bred with lep+/ob heterozygous mice (Jackson Laboratory, No. 000632) to generate ACC dLKO;lep+/ob mice, which were crossed to produce *ob/ob*;ACC dLKO mice. All mice were housed in colony cages with a 12 hour light/12 hour dark cycle and fed *ad libitum* Harlan Teklad Rodent Diet 2018 prior to study.

Studies were performed using 6 male wild type and 6 ACC dLKO mice fed chow ad lib, 6 male wild type and 6 ACC dLKO mice fed a western diet ad lib for 1 month, and 6 male wild type and 6 ACC dLKO mice fed a high fat diet ad lib for 4 months. Additional studies were performed in 6 male *ob/ob* and 6 *ob/ob*;ACC dLKO mice fed chow ad lib.

Dietary PUFA Supplementation in Mice—Purified arachidonic acid (ARA) and docosahexaenoic acid (DHA) were purchased from Nu-Chek prep. For diet studies, each was mixed into a powdered chow diet as arachidonic acid (1% w/w) and docosahexaenoic acid (0.4% w/w). Wild type and ACC dLKO (n=6 per group) male mice were fed chow or chow supplemented with 1% (wt/wt) ARA and 0.4% (wt/wt) DHA. The diet was fed to mice for 10 days and diet synchronization performed (12 hour fast/12 hour refeeding) for the last 3 days. Mice were euthanized at the end of dark cycle of the third day of diet training. High fat and high sucrose, western, and high fat diets were purchased from Research Diets (Cat. No. D12451, D12079B, and D12492, respectively).

***In Vivo* VLDL Secretion—**Wild type and ACC dLKO male mice (6 mice per group) were fasted for 2 hours and 500 mg/kg Triton WR 1339 was injected to mouse intravenously. After injection, blood was drawn at 0 minutes, 30 minutes, 1 hour, and 2 hours and TGs were measured in plasma.

GPAT1 Knockdown—(E) Sequence of siGPAT1: 5'-CACAAUAGACGUUUCUUAUCU-3' (sense) and 5'-AGAUAAGAAACGUCUAUUGUGCC-3' (antisense). For *in vivo* experiments, siRNA oligos were formulated in lipid nanoparticles (LNP) (Frank-Kamenetsky et al., 2008). GPAT1 siRNA nanoparticles were obtained from Alnylam and were formulated as previously described (Moon et al., 2012). Saline or siRNA nanoparticles directed against GPAT1 (7.5 mg/kg) was administered to wild type and ACC dLKO mice (6 male mice per

group) by subcutaneous injection. Mice were sacrificed 2 weeks after injection and livers were harvested and total RNA extracted for quantitative RT-PCR.

Measurements of Fatty Acid Synthesis in Mice—For *in vivo* studies, wild type and ACC dLKO male mice (10 mice per group) were injected intraperitoneally with [^{3}H] H_2O (50 mCi in 0.2 ml of saline) and ^{3}H incorporation into newly synthesized fatty acids were measured as described (Shimano et al., 1996).

Human Models

DNL in Humans Given MK-4074: Healthy subjects (n=11) were administered a single dose (140 mg), or divided doses (70 mg b.i.d.) of MK-4074 for 7 days and fructose-stimulated DNL assay was measured with stable isotope (^{13}C-acetate) as described below.

DNL was determined by incorporation of sodium [1-^{13}C] acetate, a stable isotopic tracer, into palmitate moiety in circulating very low density lipoprotein (VLDL)-TG. The stable isotopic tracer was intravenously infused (9–10 mg/min/man) for 19 hours and fructose was orally given to subjects every 30 min (~10 mg/kg/min fat-free mass) for the next 9.5 hours to increase baseline DNL. Blood samples were obtained hourly post start of fructose challenge. ^{13}C-labeled palmitate in VLDL fraction was isolated from blood samples and measured by LC/MS. The fraction of VLDL palmitate synthesized through the DNL pathway (fractional DNL) was calculated by using mass-isotopomer distribution analysis MIDA and the fractional contribution from DNL to the VLDL fatty acids calculated based on the precursor-product relationship (Hellerstein, 1999; Hellerstein and Neese, 1992; Hellerstein et al., 1996).

Plasma Ketones in Humans Given MK-4074—A single dose of MK-4074 (200 mg) was administered to healthy subjects (n=12) after an overnight (8-hour) fast. Pre-dose ketone bodies were obtained, followed immediately by MK-4074 dosing. Ketone bodies were then measured under fasted state (fasted) at 2, 3, 4, 5, 6, 7, and 8 hours after MK-4074 dosing. To determine ketone bodies under fed state (Fed), all subjects were given a breakfast at 1.5 hours after MK-4074 dosing and ketone bodies measured at 3, 4, 5, 6, 7, and 8 hours after MK-4074 dosing.

ACC Inhibition in Humans with NAFLD—A double-blind, randomized, placebo- and active-controlled parallel group study was designed to evaluate the effect of multiple-dose administration of MK-4074 (or matching placebo) compared to pioglitazone (or matching placebo), on changes in hepatic fat in subjects with elevated hepatic fat content. Thirty one subjects were randomized to each of 3 treatment groups and thirty subjects completed the trial: 1) twice daily 200 mg doses of MK-4074; 2) once daily 30 mg doses of pioglitazone; or 3) placebo for 4 weeks according to a computer generated allocation schedule. One subject withdrew from treatment with pioglitazone. Hepatic fat content was assessed using magnetic resonance imaging (MRI) prior to first dose administration and following 4 weeks of treatment. Thirty male subjects or female subjects (of non-childbearing potential) between the ages of 18 and 60, and with a BMI ≥32.0 kg/m^2 were recruited for this study.

Additional inclusion criteria include stable weight (by history) for at least 4 weeks prior to the study and that subjects had a baseline hepatic fat content ≥10% (as assessed by MRI).

Subjects were pre-screened by hepatic ultrasound, and only those subjects with a rating of 'moderate' or 'severe' steatosis on ultrasound were further evaluated by hepatic MRI. Subjects with a serum ALT greater than the upper limit of normal range but less than 3-fold higher than the upper limit of normal range were considered to be eligible provided that there was no known liver disease other than fatty liver or non-alcoholic steatohepatitis (NASH) (e.g., cirrhosis, viral hepatitis, autoimmune hepatitis, drug or alcohol-induced hepatitis, hemochromatosis, hepatocellular carcinoma). Subjects who had an ALT or AST ≥ 3x the upper limit of normal range (as defined by the local laboratory) at the prestudy (screening) visit were excluded. Subjects with a fasting plasma TGs level >600 mg/dL at screening were also excluded. The exploratory trial was registered as NCT01431521, “Study of Changes in Hepatic Fat Following Administration of MK-4074 and Pioglitazone Hydrochloride (MK-4074-008).” The trial was IRB approved and informed consent was obtained prior to enrollment. The study did include men and women but the sample size of each was too small to determine if there is a gender related response.

Table showing baseline characteristics of those enrolled in the trial.

Drug	**MK-4074**	**Placebo for MK-4074**	**Pioglitazone**	**Placebo for Pioglitazone**	**Total**
Overall Participants Analyzed [Number]	**10**	**5**	**11**	**5**	**31**
Age [Years] Mean (Standard Deviation)	**35.1 (5.8)**	**48.0 (7.6)**	**43.7 (12.1)**	**47.8 (10.6)**	**42.3 (10.5)**
Female	**0** (0.0%)	**1** (20.0%)	**2** (18.2%)	**4** (80.0%)	**7** (22.6%)
Male	**10** (100.0%)	**4** (80.0%)	**9** (81.8%)	**1** (20.0%)	**24** (77.4%)

The following is a detailed list of inclusion and exclusion criteria for the trial.

Inclusion Criteria

- Females must be of non-childbearing potential
- Body mass index (BMI) ≥32.0 kg/m^2
- In good health based on medical history, physical examination, vital sign measurements, and laboratory safety tests
- No clinically significant abnormality on electrocardiogram
- Has documented hepatic fat content ≥10% within 6 months of enrollment
- Maintained stable weight (by history) for at least 4 weeks
- Agrees not to initiate a weight loss program and agrees to maintain consistent dietary habits and exercise routines for the duration of the study
- Has a rating of 'moderate' or 'severe' steatosis on ultrasound at the prestudy (screening) visit

Exclusion Criteria

- Change in weight greater than 4% between prestudy visit and randomization into the study
- History of any illness that, in the opinion of the study investigator, might confound the results of the study or poses an additional risk to the participant
- Liver disease other than fatty liver or non-alcoholic steatohepatitis (NASH)
- Alanine aminotransferase (ALT) or aspartate aminotransferase (AST) ≥3x the upper limit of normal range
- Serum triglyceride level >600 mg/dL
- History of stroke, chronic seizures, or major neurological disorder
- History of clinically significant endocrine, gastrointestinal, cardiovascular (including congestive heart failure), hematological, hepatic, immunological, renal, respiratory, or genitourinary abnormalities or diseases
- Had abdominal surgery, gastric bypass, bowel resection, recent liver biopsy, or any other procedure within a minimum of 4 weeks
- History of neoplastic disease
- Claustrophobia or other contraindication to magnetic resonance imaging (MRI)
- Have not washed off agents associated with changes in hepatic fat or used for treatment of Nonalcoholic fatty liver disease (NAFLD) or NASH for a minimum of 3 months prior
- Consumes excessive amounts of alcohol, coffee, tea, cola, or other caffeinated beverages
- Had major surgery, donated or lost 1 unit of blood (approximately 500 mL) or participated in another investigational study within 4 weeks
- Significant multiple and/or severe allergies
- Intolerance or hypersensitivity to pioglitazone hydrochloride or any inactive ingredients
- Regular user of any illicit drugs or has a history of drug (including alcohol) abuse.

Additional details of the study can be found at https://clinicaltrials.gov/ct2/show/results/NCT01431521?sect=X4301256#othr.

Hepatic Fat Imaging—MRI using the 3 point Dixon method was recently qualified for use in the proof of concept study and the methods and findings have been previously described (Mashhood et al., 2013). Briefly, the 3-point Dixon or LIPOQuant MRI methods were both determined to be highly reproducible, accurate and suitable for multicenter trials to assess hepatic fat fraction; however, the 3-point Dixon method is preferred because it is simpler to implement and this approach was employed in the current study. The between-

subject CV for the 3-point Dixon method from the pilot study (ibid) was estimated to be 32%. To evaluate changes in fat fraction due to treatment with MK-4074 or pioglitazone compared to placebo, a parallel group study will be employed. The sample sizes per group required to have 80% power to detect treatment effects of 20%, 30%, 40%, and 50%, with an α=0.05 1-sided test are 37, 19, 12, and 9, respectively, assuming a between-subject CV of 32% as was observed for the 3-point Dixon method.

Measurements of Fatty Acid Synthesis in Hepatocytes—Primary hepatocytes from wild type, ACC1 LKO, ACC2 LKO, and ACC dLKO mouse livers were prepared as described (Matsuda et al., 2001). Each group of primary hepatocytes was prepared from 3 mice and plated in 6-well dishes. Dishes were set up in triplicate. [^{3}H]acetate was added to medium and cells were harvested after 3 hours of incubation. Lipids were extracted from cells using chloroform/methanol (2:1). TG and phospholipid fractions were separated using an aminopropyl column from Biotage. The rates of fatty acid synthesis was measured in the TG and phospholipid fractions by determining [^{3}H]acetate incorporation.

METHOD DETAILS

Biochemical and Cellular Assays—Recombinant ACC protein was purified from FM3A or Sf9 cells expressing recombinant ACC by chelating chromatography or from liver by Softlink avidin resin chromatography. Purified ACC protein was incubated with MK-4074 in assay buffer containing 5 mM ATP, 250 μM acetyl-CoA, 4.1 mM $NaHCO_3$, 0.086 mM $NaH14CO_3$, 20 mM potassium citrate, 20 mM MgCl2, 2 mM DTT, 0.5 mg/mL BSA and 50 mM Hepes-Na (pH 7.5) for 40 min at 37°C. For cellular assays of DNL and FAO, cells were pre-incubated with MK-4074 for 1 hour. Then the cells were incubated for additional 1–3 hours with either 65 ~ 260 μM ^{14}C-labeled acetate or 0.018 μM ^{3}H-labeled palmitate for DNL or FAO assay, respectively. After incubation, intracellular ^{14}C-labeled lipids and released ^{3}H-labeled fatty acids were extracted and measured for DNL and FAO, respectively.

Metabolite Measurements—Plasma from mouse blood was prepared by centrifuging whole blood in an EDTA tube (Microvette, Sarstedt) at 10,000 x g for 5 min. Plasma TG and cholesterol concentrations were measured using an infinity kit from ThermoFisher. Plasma ketone bodies and NEFA concentrations were measured using assays from Wako Diagnostics. Liver TGs and cholesterol concentrations were measured as described (Engelking et al., 2004). Plasma lipoproteins were separated by FPLC; cholesterol and TGs were measured as described (Horton et al., 1999).

Malonyl-CoA Measurements—The extraction of short-chain acyl-CoAs from liver were prepared as previously described (Minkler et al., 2006) with slight modifications. Approximately 50 mg of freeze-clamp frozen livers samples from wild type (8 male mice) and ACC dLKO (9 male mice) were harvested and homogenized in 500 μl ice-cold 10% trichloroacetic acid and immediately spiked with labeled [$^{13}C_3$]malonyl-CoA internal standard. Samples were centrifuged at 4°C for 10 minutes and 150 μL supernatant was loaded on an Oasis HLB lcc-30mg solid-phase extraction column. The column was washed

with water and methanol. The eluent was lyophilized and dissolved in 50 μL of mobile phase of which 1μl was subjected to LC/MS/MS analyses.

Analysis was performed on an API 3200 triple quadrupole LC/MS/MS mass spectrometer (Applied Biosystems/Sciex Instruments) in positive electrospray ionization mode. The mass spectrometer was equipped with a Shimadzu LC-20AD liquid chromatograph (LC) and a SIL-20ACHT auto sampler. Chromatography was performed on a reverse-phase C18 column (Waters xBridge, 150 × 2.1 mm, 3 μm) with a mobile phase consisting of water/methanol (95:5, v/v) and 4mM dibutylamine acetate (eluent A), and water/acetonitrile (25:75, v/v) (eluent B). Multi-reaction monitoring (MRM) was carried out for the detection of the short-chain acyl-CoAs in standard solutions and biological samples. Malonyl-CoA was quantitated by comparison of the individual ion peak area with that of the internal standard. The analytical data were processed by Analyst Software (version 1.6.2).

Quantitative Real-time PCR—Total RNA was extracted using RNA stat-60 and the RNA was treated with DNase with DNA-free kit. cDNA was synthesized using TaqMan Reverse Transcription Reagent kit. Quantitative PCR was performed as described (Liang et al., 2002). The Key Resources Table contains a complete list of the oligos used.

ACC1 and ACC2 Antibodies—For the generation of the mouse ACC1 rabbit polyclonal antibody, a cDNA encoding the N-terminal 95 amino acids from mouse ACC1 was cloned into a pGEX 4T-1 vector and the recombinant protein was expressed in *E.coli*. The purified GST-fusion protein was injected into rabbits as described (Shimano et al., 1996). For the mouse ACC2 rabbit polyclonal antibody, a cDNA encoding the N-terminal 200 amino acids of mouse ACC2 was cloned into pGEX 4T-1. After its expression in *E.coli* and purification using Ni-NTA resin, the purified protein was injected into rabbit as described (Shimano et al., 1996).

Liver Immunoblot Analysis—Livers samples (~100 mg) from frozen tissue of the indicated study were homogenized using 1 ml of buffer A (40 mM HEPES pH 7.5, 250 mM Sucrose, 1 mM EDTA, and a protease inhibitor cocktail from Thermo). Whole lysate was centrifuged at 1000 x g for 10 min to sediment the nuclear fraction and the supernatant was centrifuged again at 100,000 x g for 30 min to separate the cytosol and crude ER membrane fractions. ER membrane fractions were solubilized using 20 mM Tris pH 6.8, 1% SDS, and 50 mM NaCl. Isolated nuclear fractions were resuspended in 20 mM HEPES pH 7.5, 450 mM NaCl, with protease inhibitors to extract nuclear proteins. Equal aliquots of protein from each liver were pooled (total, 20 μg for membranes and 30 μg for nuclear extracts) and subjected to 8% SDS-PAGE and immunoblot analyses as described previously (Engelking et al., 2004; Matsuda et al., 2001; Shimano et al., 1997).

Fatty Acid Composition Measurements—Mouse liver was extracted with chloroform:methanol (2:1) and dried under nitrogen gas. Fatty acid composition was measured using gas chromatography as described previously (Moon et al., 2009).

Histology—Liver tissue sections were fixed in 10% (v/v) neutral buffered saline. Paraffin embedding, sectioning as well as hematoxylin and eosin (H&E), Oil Red O (ORO) staining was performed by the University of Texas Southwestern Molecular Pathology Core.

QUANTIFICATION AND STATISTICAL ANALYSIS

The effect of multiple doses of MK-4074 and pioglitazone on the pharmacodynamic (PD) endpoints with respect to placebo was assessed using a constrained longitudinal data analysis (cLDA) method proposed by Liang and Zeger (Liang and Zeger, 2000). This model assumes a common mean across treatment groups at baseline and a different mean for each treatment at each of the post-baseline time points. In this model, the response vector consisted of baseline and percent change (or change where applicable) from baseline at each post-baseline time point. For primary analysis the model described above was utilized for assessing the effect of MK-4074 on percent change in hepatic fat fraction from baseline with respect to placebo. Percent change in hepatic fat fraction from baseline was calculated for each of the nine liver regions separately and then these were averaged to calculate overall percent change from baseline for each subject. Baseline is defined as the mean of the hepatic fat fractions measured over all nine regions on day −1 for each subject. For the analysis the placebo groups were combined across treatments (2 and 4) as listed previously. Ninety percent (90%) confidence interval (CI) for the percent change in hepatic fat fraction from baseline in least-square means difference (MK-4074-placebo) was calculated at week 4. If the upper limit of this CI were to be <0.00 then it would be concluded that multiple-dose administration of MK-4074 caused a significant reduction in hepatic fat, thus supporting the primary hypothesis. Statistical analysis used in animal and primary hepatocyte studies can be found in the figure legends.

Supplementary Material

Refer to Web version on PubMed Central for supplementary material.

Acknowledgments

We thank Tuyet Dang, Marcus Thornton, and Judy Sanchez, for excellent technical assistance. This work was supported by grants from the National Institutes of Health HL-20948 and the Leducq Foundation. Carol Addy, Jun Kunsunoki, Cai Li, Manu Chakravarthy, Steve Previs, and David E. Kelley were employees of Merck when studies were designed and performed. Stuart Milstein and Kevin Fitzgerald are employees of Alnylam.

References

Aarsland A, Chinkes D, Wolfe RR. Hepatic and whole-body fat synthesis in humans during carbohydrate overfeeding. Am. J. Clin. Nutr. 1997; 65:1774–1782. [PubMed: 9174472]

Abu-Elheiga L, Brinkley WR, Zhong L, Chirala SS, Woldegiorgis G, Wakil SJ. The subcellular localization of acetyl-CoA carboxylase 2. Proc. Natl. Acad. Sci. U. S. A. 2000; 97:1444–1449. [PubMed: 10677481]

Abu-Elheiga L, Matzuk MM, Abo-Hashema KAH, Wakil SJ. Continuous fatty acid oxidation and reduced fat storage in mice lacking acetyl-CoA carboxylase 2. Science. 2001; 291:2613–2616. [PubMed: 11283375]

Abu-Elheiga L, Matzuk MM, Kordari P, Oh W, Shaikenov T, Gu Z, Wakil SJ. Mutant mice lacking acetyl-CoA carboxylase 1 are embryonically lethal. Proc. Natl. Acad. Sci. U. S. A. 2005; 102:12011–12016. [PubMed: 16103361]

Abu-Elheiga L, Oh W, Kordari P, Wakil SJ. Acetyl-CoA carboxylase 2 mutant mice are protected against obesity and diabetes induced by high-fat/high-carbohydrate diets. Proc. Natl. Acad. Sci. U. S. A. 2003; 100:10207–10212. [PubMed: 12920182]

Araujo S, Soares ESA, Gomes F, Ribeiro E, Oliveira W, Oliveira A, Lima I, Lima Mdo C, Pitta I, Peixoto C. Effects of the new thiazolidine derivative LPSF/GQ-02 on hepatic lipid metabolism pathways in non-alcoholic fatty liver disease (NAFLD). Eur. J. Pharmacol. 2016; 788:306–314. [PubMed: 27349145]

Bajaj M, Suraamornkul S, Pratipanawatr T, Hardies LJ, Pratipanawatr W, Glass L, Cersosimo E, Miyazaki Y, DeFronzo RA. Pioglitazone reduces hepatic fat content and augments splanchnic glucose uptake in patients with type 2 diabetes. Diabetes. 2003; 52:1364–1370. [PubMed: 12765945]

Belfort R, Harrison SA, Brown K, Darland C, Finch J, Hardies J, Balas B, Gastaldelli A, Tio F, Pulcini J, et al. A placebo-controlled trial of pioglitazone in subjects with nonalcoholic steatohepatitis. The New England journal of medicine. 2006; 355:2297–2307. [PubMed: 17135584]

Bell LN, Wang J, Muralidharan S, Chalasani S, Fullenkamp AM, Wilson LA, Sanyal AJ, Kowdley KV, Neuschwander-Tetri BA, Brunt EM, et al. Relationship between adipose tissue insulin resistance and liver histology in nonalcoholic steatohepatitis: a pioglitazone versus vitamin E versus placebo for the treatment of nondiabetic patients with nonalcoholic steatohepatitis trial follow-up study. Hepatology. 2012; 56:1311–1318. [PubMed: 22532269]

Browning JD, Horton JD. Molecular mediators of hepatic steatosis and liver injury. J. Clin. Invest. 2004; 114:147–152. [PubMed: 15254578]

Browning JD, Szczepaniak LS, Dobbins R, Nuremberg P, Horton JD, Cohen JC, Grundy SM, Hobbs HH. Prevalence of hepatic steatosis in an urban population in the United States: Impact of ethnicity. Hepatology. 2004; 40:1387–1395. [PubMed: 15565570]

Chakravarthy MV, Lodhi IJ, Yin L, Malapaka RR, Xu HE, Turk J, Semenkovich CF. Identification of a physiologically relevant endogenous ligand for PPARalpha in liver. Cell. 2009; 138:476–488. [PubMed: 19646743]

Chakravarthy MV, Pan Z, Zhu Y, Tordjman K, Schneider JG, Coleman T, Turk J, Semenkovich CF. "New" hepatic fat activates PPARαlpha to maintain glucose, lipid, and cholesterol homeostasis. Cell Metab. 2005; 1:309–322. [PubMed: 16054078]

Chalasani N, Younossi Z, Lavine JE, Diehl AM, Brunt EM, Cusi K, Charlton M, Sanyal AJ. The diagnosis and management of non-alcoholic fatty liver disease: practice guideline by the American Gastroenterological Association, American Association for the Study of Liver Diseases, and American College of Gastroenterology. Gastroenterology. 2012; 142:1592–1609. [PubMed: 22656328]

Choi CS, Savage DB, Abu-Elheiga L, Liu ZX, Kim S, Kulkarni A, Distefano A, Hwang YJ, Reznick RM, Codella R, et al. Continuous fat oxidation in acetyl-CoA carboxylase 2 knockout mice increases total energy expenditure, reduces fat mass, and improves insulin sensitivity. Proc. Natl. Acad. Sci. U. S. A. 2007; 104:16480–16485. [PubMed: 17923673]

Cohen JC, Horton JD, Hobbs HH. Human fatty liver disease: old questions and new insights. Science. 2011; 332:1519–1523. [PubMed: 21700865]

Cusi K, Orsak B, Bril F, Lomonaco R, Hecht J, Ortiz-Lopez C, Tio F, Hardies J, Darland C, Musi N, et al. Long-Term Pioglitazone Treatment for Patients With Nonalcoholic Steatohepatitis and Prediabetes or Type 2 Diabetes Mellitus: A Randomized Trial. Ann. Intern Med. 2016; 165:305–315. [PubMed: 27322798]

Donnelly KL, Smith CI, Schwarzenberg SJ, Jessurun J, Boldt MD, Parks EJ. Sources of fatty acids stored in liver and secreted via lipoproteins in patients with nonalcoholic fatty liver disease. J. Clin. Invest. 2005; 115:1343–1351. [PubMed: 15864352]

Engelking LJ, Kuriyama H, Hammer RE, Horton JD, Brown MS, Goldstein JL, Liang G. Overexpression of Insig-1 in the livers of transgenic mice inhibits SREBP processing and reduces insulin-stimulated lipogenesis. J. Clin. Invest. 2004; 113:1168–1175. [PubMed: 15085196]

Fabbrini E, Mohammed BS, Magkos F, Korenblat KM, Patterson BW, Klein S. Alterations in adipose tissue and hepatic lipid kinetics in obese men and women with nonalcoholic fatty liver disease. Gastroenterology. 2008; 134:424–431. [PubMed: 18242210]

Frank-Kamenetsky M, Grefhorst A, Anderson NN, Racie TS, Bramlage B, Akinc A, Butler D, Charisse K, Dorkin R, Fan Y, et al. Therapeutic RNAi targeting PCSK9 acutely lowers plasma cholesterol in rodents and LDL cholesterol in nonhuman primates. Proc Natl Acad Sci U S A. 2008; 105:11915–11920. [PubMed: 18695239]

Gonzalez-Baro MR, Lewin TM, Coleman RA. Regulation of Triglyceride Metabolism. II. Function of mitochondrial GPAT1 in the regulation of triacylglycerol biosynthesis and insulin action. Am. J. Physiol. Gastrointest. Liver Physiol. 2007; 292:G1195–1199. [PubMed: 17158253]

Grefhorst A, McNutt MC, Lagace TA, Horton JD. Plasma PCSK9 preferentially reduces liver LDL receptors in mice. J. Lipid Res. 2008; 49:1303–1311. [PubMed: 18354138]

Grundy SM, Brewer HB Jr, Cleeman JI, Smith SC Jr, Lenfant C. Definition of metabolic syndrome: Report of the National Heart, Lung, and Blood Institute/American Heart Association conference on scientific issues related to definition. Circulation. 2004; 109:433–438. [PubMed: 14744958]

Harada N, Oda Z, Hara Y, Fujinami K, Okawa M, Ohbuchi K, Yonemoto M, Ikeda Y, Ohwaki K, Aragane K, et al. Hepatic de novo lipogenesis is present in liver-specific ACC1-deficient mice. Mol. Cell Biol. 2007; 27:1881–1888. [PubMed: 17210641]

Harriman G, Greenwood J, Bhat S, Huang X, Wang R, Paul D, Tong L, Saha AK, Westlin WF, Kapeller R, et al. Acetyl-CoA carboxylase inhibition by ND-630 reduces hepatic steatosis, improves insulin sensitivity, and modulates dyslipidemia in rats. Proc. Natl. Acad. Sci. U. S. A. 2016; 113:E1796–1805. [PubMed: 26976583]

He S, McPhaul C, Li JZ, Garuti R, Kinch L, Grishin NV, Cohen JC, Hobbs HH. A sequence variation (I148M) in PNPLA3 associated with nonalcoholic fatty liver disease disrupts triglyceride hydrolysis. J. Biol. Chem. 2010; 285:6706–6715. [PubMed: 20034933]

Hellerstein MK. De novo lipogenesis in humans: metabolic and regulatory aspects. Eur. J. Clin. Nutr. 1999; 53:S53–65. [PubMed: 10365981]

Hellerstein MK, Neese RA. Mass isotopomer distribution analysis: a technique for measuring biosynthesis and turnover of polymers. Am. J. Physiol. 1992; 263:E988–1001. [PubMed: 1443132]

Hellerstein MK, Schwarz JM, Neese RA. Regulation of hepatic de novo lipogenesis in humans. Annu. Rev. Nutr. 1996; 16:523–557. [PubMed: 8839937]

Horton JD, Goldstein JL, Brown MS. SREBPs:activators of the complete program of cholesterol and fatty acid synthesis in the liver. J. Clin. Invest. 2002; 109:1125–1131. [PubMed: 11994399]

Horton JD, Shimano H, Hamilton RL, Brown MS, Goldstein JL. Disruption of LDL receptor gene in transgenic SREBP-1a mice unmasks hyperlipidemia resulting from production of lipid-rich VLDL. J. Clin. Invest. 1999; 103:1067–1076. [PubMed: 10194480]

Huang Y, He S, Li JZ, Seo YK, Osborne TF, Cohen JC, Hobbs HH. A feed-forward loop amplifies nutritional regulation of PNPLA3. Proc. Natl. Acad. Sci. U. S. A. 2010; 107:7892–7897. [PubMed: 20385813]

Hudgins LC, Hellerstein MK, Seidman CE, Neese RA, Tremaroli JD, Hirsch J. Relationship between carbohydrate-induced hypertriglyceridemia and fatty acid synthesis in lean and obese subjects. J. Lipid Res. 2000; 41:595–604. [PubMed: 10744780]

Khan MA, St Peter JV, Xue JL. A prospective, randomized comparison of the metabolic effects of pioglitazone or rosiglitazone in patients with type 2 diabetes who were previously treated with troglitazone. Diabetes Care. 2002; 25:708–711. [PubMed: 11919129]

Lambert JE, Ramos-Roman MA, Browning JD, Parks EJ. Increased de novo lipogenesis is a distinct characteristic of individuals with nonalcoholic fatty liver disease. Gastroenterology. 2014; 146:726–735. [PubMed: 24316260]

Li JZ, Huang Y, Karaman R, Ivanova PT, Brown HA, Roddy T, Castro-Perez J, Cohen JC, Hobbs HH. Chronic overexpression of PNPLA3I148M in mouse liver causes hepatic steatosis. J. Clin. Invest. 2012; 122:4130–4144. [PubMed: 23023705]

Liang G, Yang J, Horton JD, Hammer RE, Goldstein JL, Brown MS. Diminished hepatic response to fasting/refeeding and LXR agonists in mice with selective deficiency of SREBP-1c. J. Biol. Chem. 2002; 277:9520–9528. [PubMed: 11782483]

Liang K, Zeger S. Longitudinal data analysis of continuous and discrete responses for pre-postdesigns. Sankhyā: The Indian Journal of Statistics. 2000; 62:134–148.

Mao J, DeMayo FJ, Li H, Abu-Elheiga L, Gu Z, Shaikenov TE, Kordari P, Chirala SS, Heird WC, Wakil SJ. Liver-specific deletion of acetyl-CoA carboxylase 1 reduces hepatic triglyceride accumulation without affecting glucose homeostasis. Proc. Natl. Acad. Sci. U S A. 2006; 103:8552–8557. [PubMed: 16717184]

Mashhood A, Railkar R, Yokoo T, Levin Y, Clark L, Fox-Bosetti S, Middleton MS, Riek J, Kauh E, Dardzinski BJ, et al. Reproducibility of hepatic fat fraction measurement by magnetic resonance imaging. J. Magn. Reson. Imaging. 2013; 37:1359–1370. [PubMed: 23172799]

Matsuda M, Korn BS, Hammer RE, Moon YA, Komuro R, Horton JD, Goldstein JL, Brown MS, Shimomura I. SREBP cleavage-activating protein (SCAP) is required for increased lipid synthesis in liver induced by cholesterol deprivation and insulin elevation. Genes Dev. 2001; 15:1206–1216. [PubMed: 11358865]

Minkler PE, Kerner J, Kasumov T, Parland W, Hoppel CL. Quantification of malonyl-coenzyme A in tissue specimens by high-performance liquid chromatography/mass spectrometry. Anal Biochem. 2006; 352:24–32. [PubMed: 16545769]

Moon Y-A, Horton JD. Identification of two mammalian reductases involved in the two-carbon fatty acyl elongation cascade. J. Biol. Chem. 2003; 278:7335–7343. [PubMed: 12482854]

Moon YA, Hammer RE, Horton JD. Deletion of ELOVL5 leads to fatty liver through activation of SREBP-1c in mice. J. Lipid Res. 2009; 50:412–423. [PubMed: 18838740]

Moon YA, Liang G, Xie X, Frank-Kamenetsky M, Fitzgerald K, Koteliansky V, Brown MS, Goldstein JL, Horton JD. The Scap/SREBP pathway is essential for developing diabetic fatty liver and carbohydrate-induced hypertriglyceridemia in animals. Cell Metab. 2012; 15:240–246. [PubMed: 22326225]

Musso G, Cassader M, Paschetta E, Gambino R. Thiazolidinediones and Advanced Liver Fibrosis in Nonalcoholic Steatohepatitis: A Meta-analysis. JAMA Intern Med. 2017; 177:633–640. [PubMed: 28241279]

Musso G, Gambino R, Cassader M, Pagano G. A meta-analysis of randomized trials for the treatment of nonalcoholic fatty liver disease. Hepatology. 2010; 52:79–104. [PubMed: 20578268]

Olson DP, Pulinilkunnil T, Cline GW, Shulman GI, Lowell BB. Gene knockout of Acc2 has little effect on body weight, fat mass, or food intake. Proc. Natl. Acad. Sci. U. S. A. 2010; 107:7598–7603. [PubMed: 20368432]

Promrat K, Lutchman G, Uwaifo GI, Freedman RJ, Soza A, Heller T, Doo E, Ghany M, Premkumar A, Park Y, et al. A pilot study of pioglitazone treatment for nonalcoholic steatohepatitis. Hepatology. 2004; 39:188–196. [PubMed: 14752837]

Romeo S, Kozlitina J, Xing C, Pertsemlidis A, Cox D, Pennacchio LA, Boerwinkle E, Cohen JC, Hobbs HH. Genetic variation in PNPLA3 confers susceptibility to nonalcoholic fatty liver disease. Nat. Genet. 2008; 40:1461–1465. [PubMed: 18820647]

Sanyal AJ, Chalasani N, Kowdley KV, McCullough A, Diehl AM, Bass NM, Neuschwander-Tetri BA, Lavine JE, Tonascia J, Unalp A, et al. Pioglitazone, vitamin E, or placebo for nonalcoholic steatohepatitis. The New England journal of medicine. 2010; 362:1675–1685. [PubMed: 20427778]

Shimano H, Horton JD, Hammer RE, Shimomura I, Brown MS, Goldstein JL. Overproduction of cholesterol and fatty acids causes massive liver enlargement in transgenic mice expressing truncated SREBP-1a. J. Clin. Invest. 1996; 98:1575–1584. [PubMed: 8833906]

Shimano H, Horton JD, Shimomura I, Hammer RE, Brown MS, Goldstein JL. Isoform 1c of sterol regulatory element binding protein is less active than isoform 1a in livers of transgenic mice and in cultured cells. J. Clin. Invest. 1997; 99:846–854. [PubMed: 9062341]

Shimomura I, Bashmakov Y, Horton JD. Increased levels of nuclear SREBP-1c associated with fatty livers in two mouse models of diabetes mellitus. J. Biol. Chem. 1999a; 274:30028–30032. [PubMed: 10514488]

Shimomura I, Bashmakov Y, Ikemoto S, Horton JD, Brown MS, Goldstein JL. Insulin selectively increases SREBP-1c mRNA in the livers of rats with streptozotocin-induced diabetes. Proc. Natl. Acad. Sci. U. S. A. 1999b; 96:13656–13661. [PubMed: 10570128]

Smagris E, BasuRay S, Li J, Huang Y, Lai KM, Gromada J, Cohen JC, Hobbs HH. Pnpla3I148M knockin mice accumulate PNPLA3 on lipid droplets and develop hepatic steatosis. Hepatology. 2015; 61:108–118. [PubMed: 24917523]

Thampy KG, Wakil SJ. Regulation of acetyl-coenzyme A carboxylase. I. Purification and properties of two forms of acetyl-coenzyme A carboxylase from rat liver. J. Biol. Chem. 1988a; 263:6447–6453. [PubMed: 2896193]

Thampy KG, Wakil SJ. Regulation of acetyl-coenzyme A carboxylase. II. Effect of fasting and refeeding on the activity, phosphate content, and aggregation state of the enzyme. J. Biol. Chem. 1988b; 263:6454–6458. [PubMed: 2896194]

Wolfe R. Metabolic interactions between glucose and fatty acids in humans. Am. J. Clin. Nutr. 1998; 67:519S–526. [PubMed: 9497163]

Highlights

- Inhibition of ACC in liver reduces lipogenesis and increases fatty acid oxidation
- In humans with fatty livers, ACC inhibition reduces liver triglycerides
- Deletion of ACCs depletes malonyl-CoA, reducing polyunsaturated fatty acid synthesis
- Resulting activation of SREBP-1c increases GPAT1 leading to hypertriglyceridemia

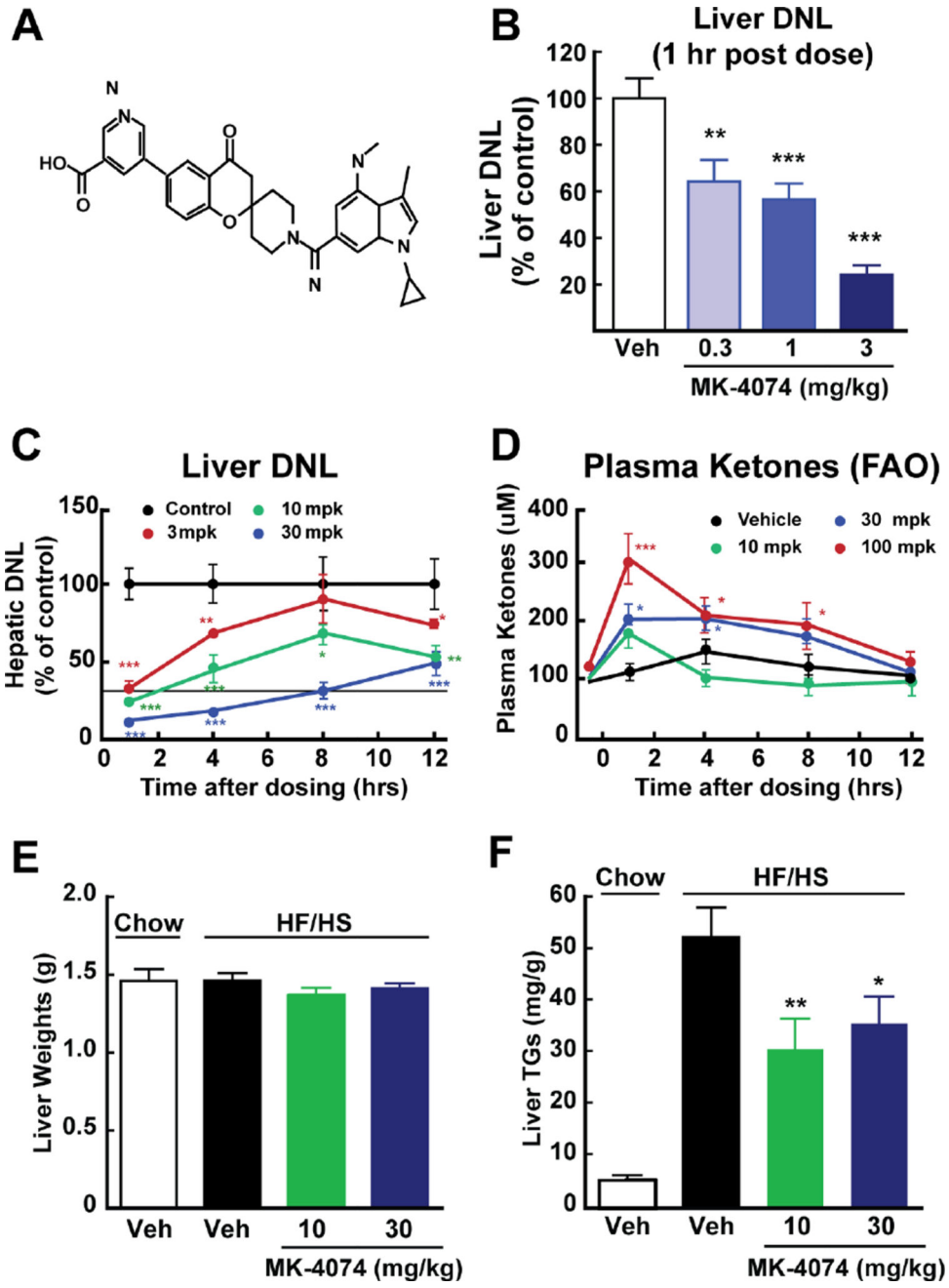

Figure 1. Liver Targeting ACC1 and ACC2 Inhibitor MK-4074

(A) Chemical structure of MK-4074.

(B) Male KKAy mice (n=10–11/group) were administered a single oral dose of MK-4074 (0.3 to 3 mg/kg) and DNL rates was measured from the liver slices as described in Experimental Procedures.

(C) Male KKAy mice (n=5/group) were administered a single oral dose of MK-4074 (3 to 30 mg/kg) and liver DNL rates were measured.

(D) Male KKAy mice (n=8/group) were administered a single oral dose of MK-4074 (10 to 100 mg/kg) and plasma ketone bodies were measured at the indicated times.

(E) Male C57BL/6J mice (n=5, veh; n=10, MK-4074) were fed chow or a high fat/high sucrose (HF/HS) diet for 7 weeks and vehicle or MK-4074 was administered orally (10 or 30 mg/kg/day) for 4 weeks. At the end of 4 weeks, mice were euthanized and liver weights obtained.

(F) Liver TG concentrations from mice described in (E).

Statistical analysis was performed with Williams test except for Figure 1E, which used a two-tailed Student's t test (* denotes $p<0.05$, ** denotes $p<0.01$, and *** denotes $p<0.001$).

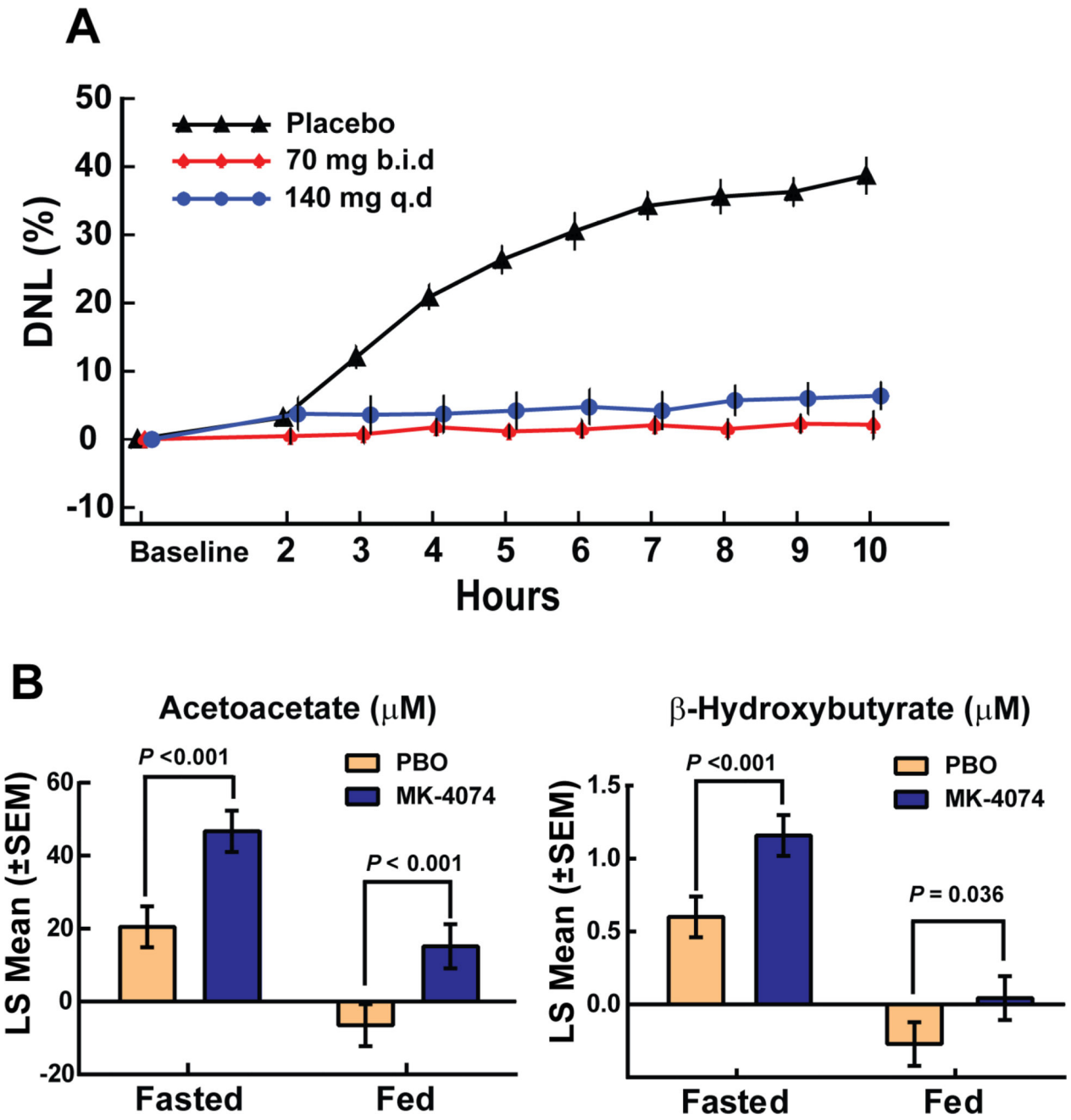

Figure 2. Phase 1 Clinical Pharmacology

(A) Healthy subjects (n=11) were administered a single dose (140 mg), or divided doses (70 mg b.i.d.) of MK-4074 for 7 days and fructose-stimulated DNL assay was measured with stable isotope (^{13}C-acetate) as described in Experimental Procedures.

(B) A single dose of MK-4074 (200 mg) was administered to healthy subjects (n=12) after an overnight (8-hour) fast. Pre-dose ketone bodies were obtained, followed immediately by MK-4074 dosing. Ketone bodies were then measured under fasted state (Fasted) at 2, 3, 4, 5, 6, 7, and 8 hours after MK-4074 dosing. To determine ketone bodies under fed state (Fed), all subjects were given a breakfast at 1.5 hours after MK-4074 dosing and ketone bodies

measured at 3, 4, 5, 6, 7, and 8 hours after MK-4074 dosing. The least square geometric mean change from pre-dose in acetoacetate and β-hydroxybutyrate plasma concentrations were plotted.

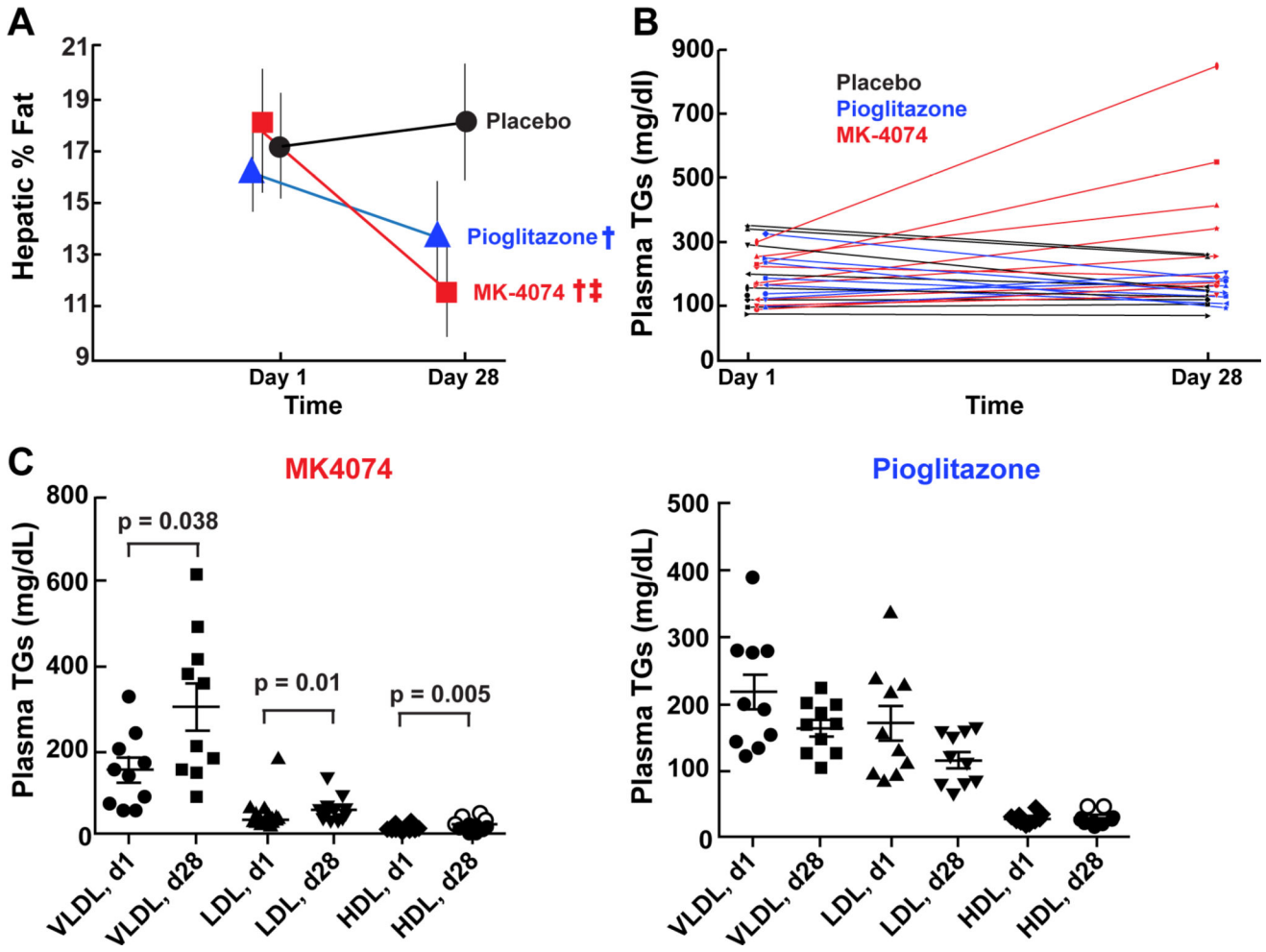

Figure 3. MK-4074 Decreased Hepatic TGs but Increased Plasma TGs in Humans

(A) Thirty male or female patients between the ages of 18 and 60 (Table S2) were randomized to: 1) twice daily 200 mg dose of MK-4074; 2) once daily pioglitazone (30 mg); or 3) placebo for 4 weeks. Hepatic TG content was assessed using magnetic resonance imaging (MRI) prior to first administration and following 4 weeks of treatment. † Statistically lower than placebo, ‡ statistically lower than pioglitazone. Statistic methods are described in Experimental Procedures and Table S3.

(B) Plasma TG concentrations from subjects described in (A).

(C) Plasma was obtained from subjects described in (A), lipoproteins were size-fractionated by FPLC, and TG content measured as described in Experimental Procedures.

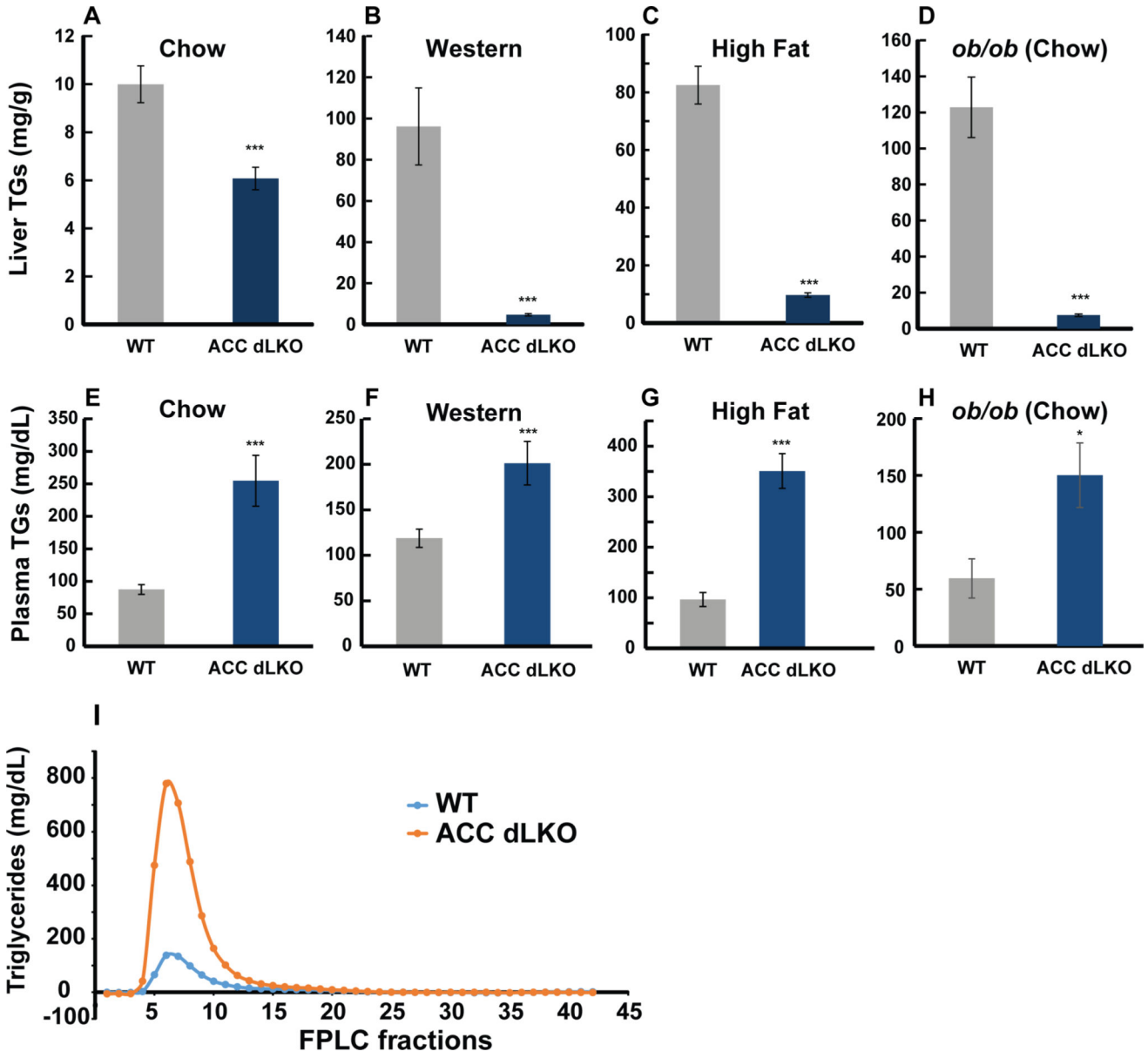

Figure 4. Liver TGs are Reduced in ACC dLKO Mice, but Plasma TGs are Elevated in ACC dLKO Mice

(A) Liver TG concentrations from 6 male wild type and 6 ACC dLKO mice fed chow ad lib.

(B) Liver TG concentrations from 6 male wild type and 6 ACC dLKO mice fed a western diet ad lib for 1 month.

(C) Liver TG concentrations from 6 male wild type and 6 ACC dLKO mice fed a high fat diet ad lib for 4 months.

(D) Liver TG concentrations from 6 male *ob/ob* and 6 *ob/ob*;ACC dLKO mice fed chow ad lib.

(E) Plasma TGs from mice in (A).

(F) Plasma TGs from mice in (B).

(G) Plasma TGs from mice in (C).

(H) Plasma TGs from mice in (D).

(I) FPLC of plasma lipoproteins of wild type and ACC dLKO mice fed chow described in (A). Pooled plasma (500 μl) was size-fractionated using a superose 6 column and TG concentrations were measured in each fraction as described in Experimental Procedures. Statistical analysis was performed using the two-tailed Student's t test (* denotes $p<0.05$, ** denotes $p<0.01$, and *** denotes $p<0.001$).

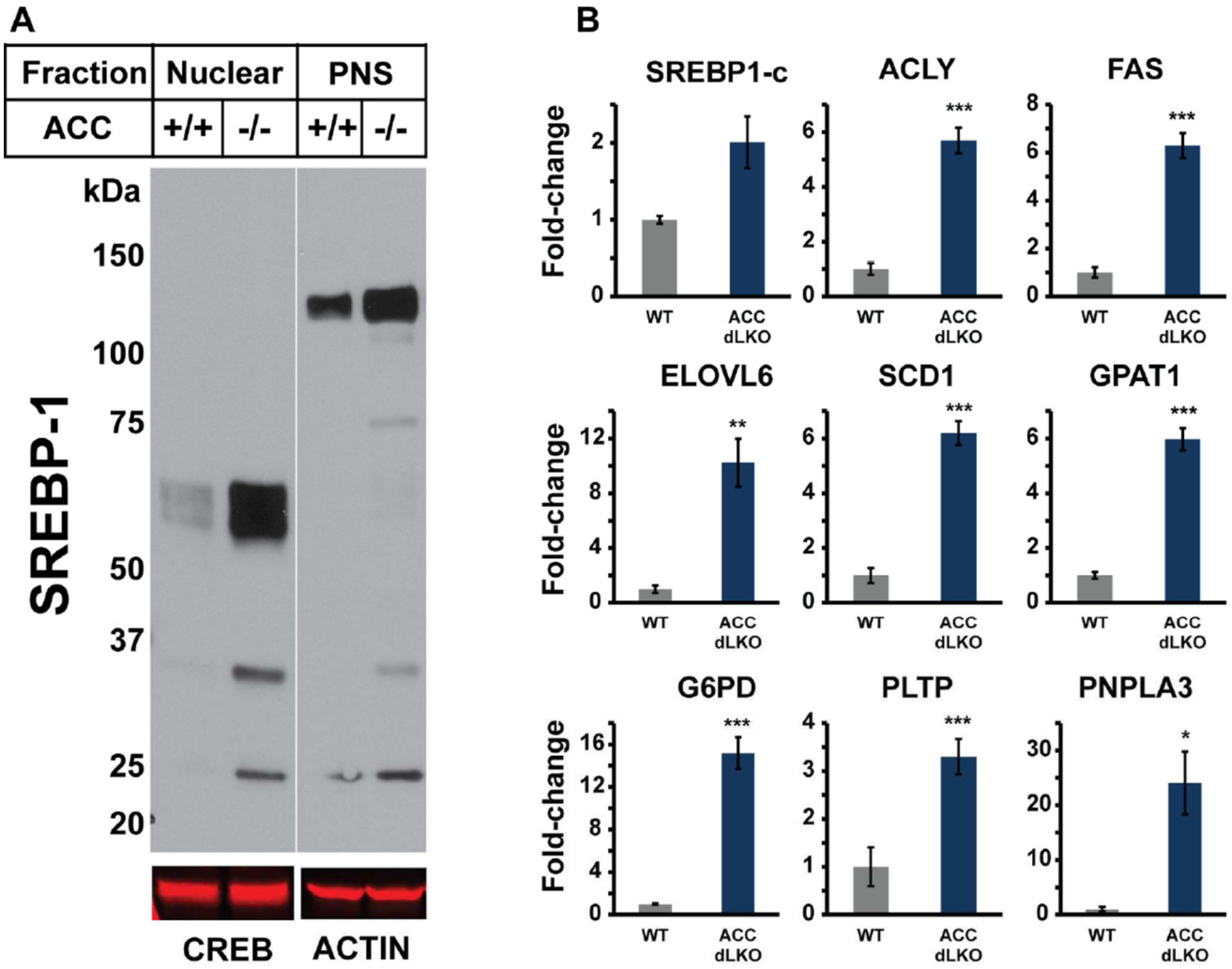

Figure 5. SREBP-1c Levels are Increased in ACC dLKO Mouse Livers

(A) Aliquots of livers (100 μg) from the mice described in Figure 4A were homogenized and nuclear and post-nuclear fractions were prepared as described in Experimental Procedures. Pooled nuclear and post-nuclear fractions (30 μg) were subjected to SDS-PAGE and immunoblot analysis was carried out using an anti-SREBP-1 rabbit monoclonal antibody.

(B) Liver RNA was prepared from the mice described in Figure 4A and quantitative PCR was performed as described in Experimental Procedures.

Statistical analysis was performed with the two-tailed Student's t test (* denotes $p<0.05$, ** denotes $p<0.01$, and *** denotes $p<0.001$).

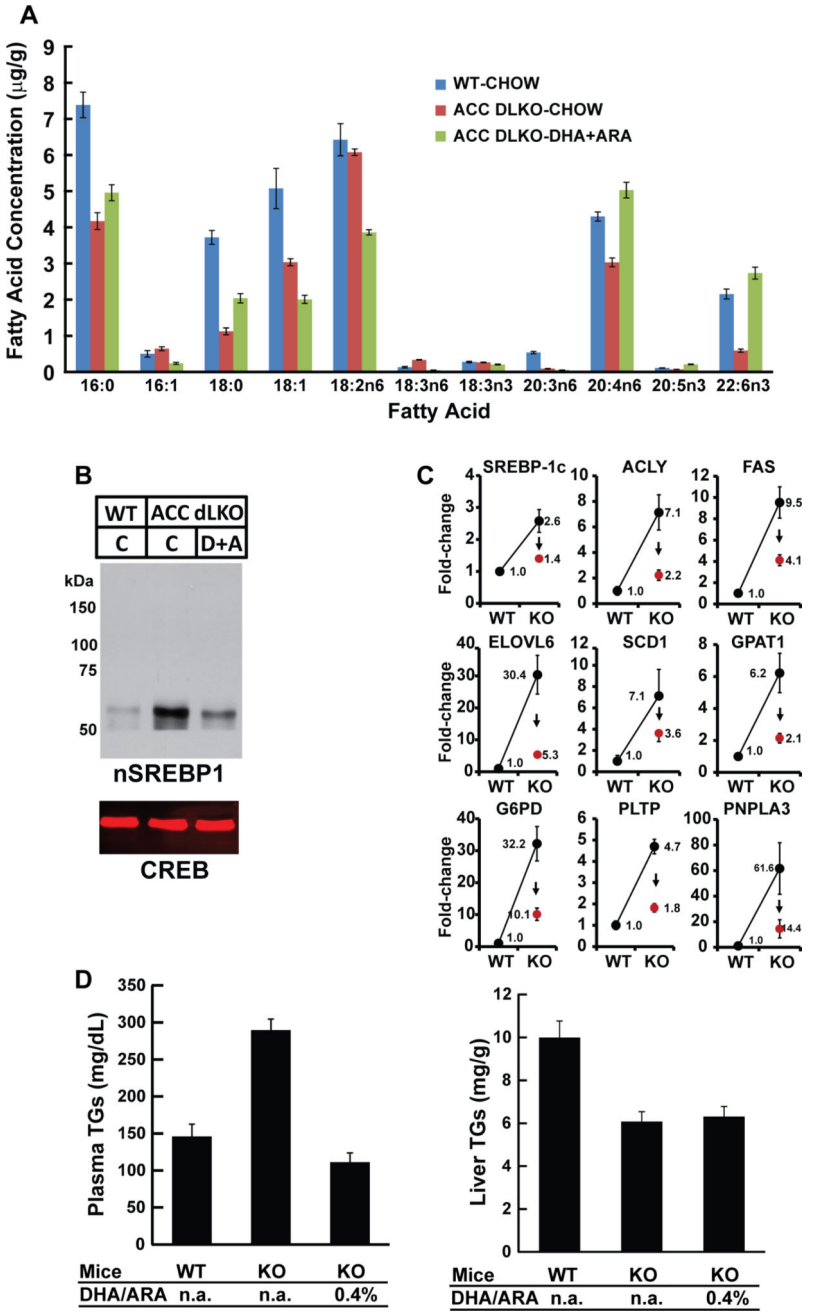

Figure 6. Dietary PUFA Supplementation Normalizes SREBP-1c in ACC dLKO Mouse Livers

(A) Wild type and ACC dLKO (n=6 per group) male mice were fed chow or chow supplemented with 1% (wt/wt) ARA and 0.4% (wt/wt) DHA. Livers were harvested and lipids were extracted and fatty acids analyzed using gas chromatography as described in Experimental Procedures.

(B) Nuclear and post nuclear fractions were prepared from each liver of mice in (A) and equal aliquots pooled (30 μg), subjected to SDS-PAGE, and immunoblot analysis carried out as described in Figure 5.

(C) Total RNA was prepared from each mouse liver in (A) and subjected to quantitative PCR as described in Experimental Procedures (Black represents chow fed group; red represents chow supplemented with ARA and DHA)
(D) Plasma TGs from mice in (A) were measured as described in Experimental Procedures.
(E) Liver TGs from mice in (A) were measured as described in Experimental Procedures.
Statistical analysis was performed with the two-tailed Student's t test.

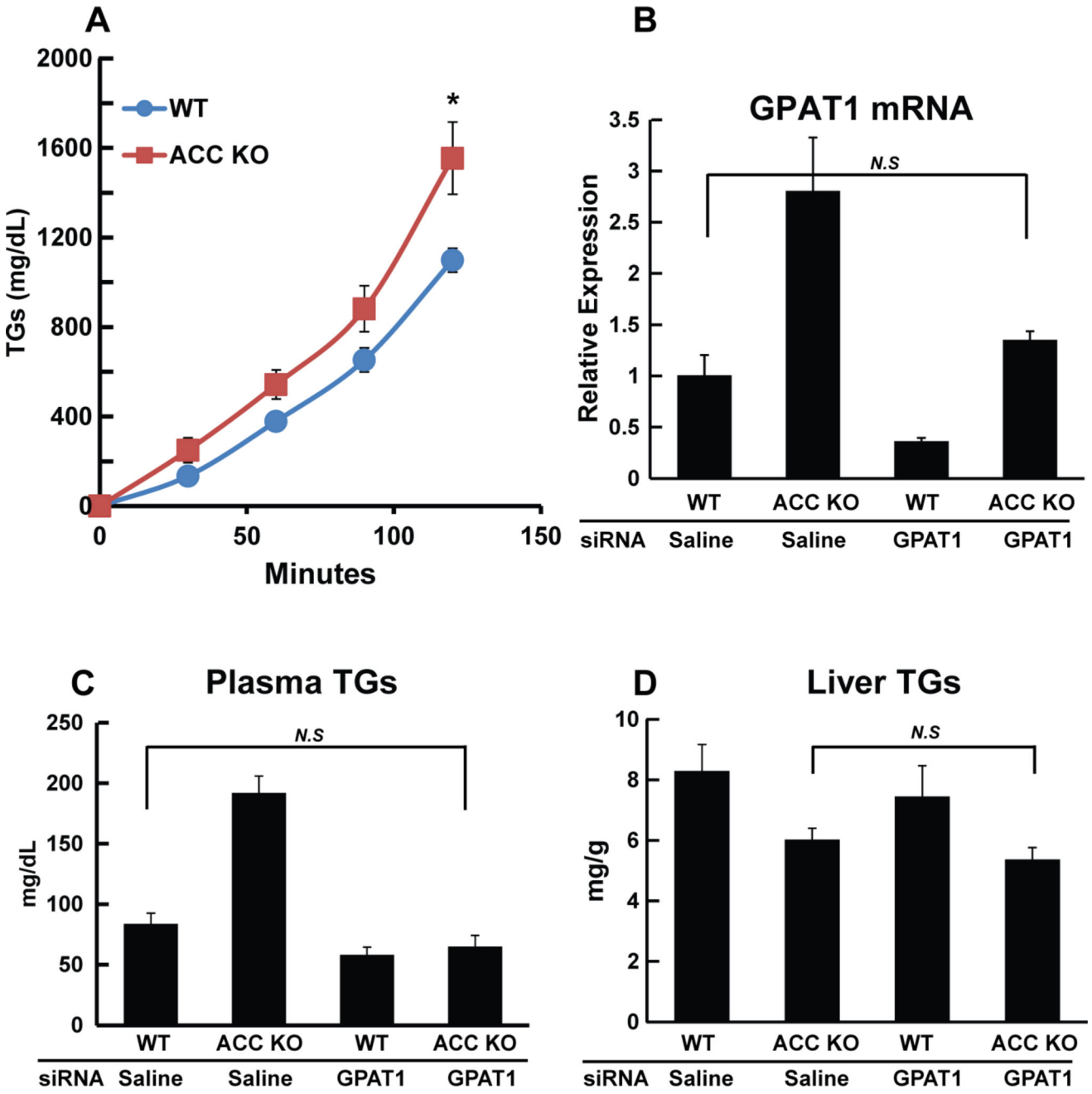

Figure 7. Liver TG Secretion from Livers of ACC dLKO Mice is Increased and Knockdown of GPAT1 Expression Normalizes Plasma TGs

(A) Wild type and ACC dLKO male mice (6 mice per group) were fasted for 2 hours and Triton WR 1339 was injected to mouse intravenously. After injection, blood was collected at 0 minutes, 30 minutes, 1 hour, and 2 hours and TGs were measured in plasma.

(B) Saline or siRNA nanoparticles directed against GPAT1 (7.5 mg/kg) was administered to wild type and ACC dLKO mice (6 male mice per group) by subcutaneous injection. Mice were sacrificed 2 weeks after injection and total RNA was extracted from each liver and GPAT1 mRNA was quantified using quantitative RT-PCR as described in Experimental Procedures.

(C) Plasma TGs were measured as described in Experimental Procedures.

(D) Liver TGs were measured as described in Experimental Procedures.

Statistical analysis was performed with the two-tailed Student's t test (* denotes $p<0.05$).